SYNTHESIS, REACTIONS AND KINETICS OF INDENYL-NITROSYL GROUP (VI) METAL CARBONYL COMPLEXES WITH PHOSPHORUS LIGANDS

A Dissertation

Presented in Partial Fulfillment of the Requirements for the

Degree of Doctor of Philosophy

with a

Major in Chemistry

in the

College of Graduate Studies

University of Idaho

by

Rmdan A. Altwer

December 2014

Major Professor: Thomas Bitterwolf, Ph.D.

AUTHORIZATION TO SUBMIT DISSERTATION

This dissertation of Rmdan A. Altwer, submitted for the degree of Doctor of Philosophy with a Major in Chemistry and titled "Synthesis, Reactions and Kinetics of Indenyl-Nitrosyl Group (VI) Metal Carbonyl Complexes with Phosphorus Ligands," has been reviewed in final form. Permission, as indicated by signatures and dates below, is now granted to submit final copies to the College of Graduate Studies for approval.

Major Professor: _____ Date _____
Thomas Bitterwolf, Ph.D.,

Committee Members: _____ Date _____
Aicha Elshabini, Ph.D., P.E.

_____ Date _____
Jakob Magolan, Ph.D.

_____ Date _____
I. Frank Chang, Ph.D.

Department Administrator: _____ Date _____
Ray von Wandruszka, Ph.D.

Dean of College Of Science: _____ Date _____
Paul Joyce, Ph.D.

Final Approval and Acceptance

Dean of the College Of Graduate Studies: _____ Date _____
Jie Chen, Ph.D.

ABSTRACT

Ligand exchange reactions between various metal carbonyl derivatives and incoming ligands such as phosphine and phosphites have been extensively studied. It is known that prototypical organometallic compounds such as $(\eta^5\text{-}C_5H_5)Mn(CO)_3$ are virtually unreactive to thermal exchange of carbonyl ligands while its indenyl derivative $(\eta^5\text{-}C_9H_7)Mn(CO)_3$ undergoes carbonyl exchange at moderate temperatures. Several examples of rate acceleration by indenyl ligands relative to cyclopentadienyl ligands have now been reported and the observed "indenyl effect" attributed to the ability of the indenyl ligand being able to shift its binding from η^5 to η^3 during associative reactions. This η^5 to η^3 haptotropic rearrangement lowers the energy of activation. A similar effect has been observed for metal nitrosyl compounds. In these cases, the nitrosyl ligand is normally observed to be bound linearly to the metal and formally treated as a three-electron donor. Associative reactions of metal carbonyl, nitrosyl compounds with ligands have been shown to be accelerated relative to all carbonyl compounds. This acceleration is attributed to a "nitrosyl effect" in which the nitrosyl ligand can go from a linear, three-electron donor to a bent, one-electron donor in the associative reaction intermediate. The family of Group VI compounds $\eta^5\text{-}C_5H_5)M(CO)_2(NO)$ and their indenyl derivatives offer an interesting platform to examine both indenyl and nitrosyl effects in the same molecules The $(\eta^5\text{-}C_5H_5)M(CO)_2(NO)$ derivatives for Cr, Mo and W are known, but only $(\eta^5\text{-}C_9H_7)Cr(CO)_2(NO)$ has been reported for the indenyl derivatives. The chromium compound was prepared using $CrCl(CO)_2(NO)Py_2$ as a precursor. This research set out to prepare the series of Group VI compounds, $(\eta^5\text{-}C_9H_7)M(CO)_2(NO)$, by conventional routes using the reaction of $(\eta^5\text{-}$

$C_9H_7)M(CO)_3$ anions with known NO donors such as Diazald. Subsequent carbonyl exchange kinetics studies were planned with the goal of investigating the indenyl and nitrosyl effects down the Group VI family of compounds. (η^5-C_9H_7)Cr(CO)$_2$(NO) was successfully prepared by the proposed route, albeit in low yield, but neither the Mo or W compounds could be prepared. A simple alkylation reaction to prepare (η^5-C_9H_7)M(CO)$_3$($CH_2C_6H_5$) was carried out after many failures to ensure ourselves that the intermediate (η^5-C_9H_7)M(CO)$_3$ anions were being successfully prepared. Our kinetics studies were therefore limited to (η^5-C_9H_7)Cr(CO)$_2$(NO). As noted above, the corresponding (η^5-C_5H_5)Cr(CO)$_2$(NO) derivative has been reported to be thermally unreactive with PPh_3 although derivatives of the form (η^5-C_5H_5)Cr(CO)(NO)L, where L = phosphine or phosphite, can be prepared photochemically. We have carried out a series of pseudo-first order kinetics studies of (η^5-C_9H_7)Cr(CO)$_2$(NO) with PMe_3, PBu_3, PMe_2Ph and $P(OMe)_3$. This series represents a range of ligand nucleophilicity and cone angle (steric bulk). Energies of activation were determined by measurements of the rates of reaction across a range of temperatures, while the entropy and enthalpies of activation were extracted from Eyring plots. The strongly negative entropies of activation are consistent with an associative reaction. The data do not allow us to parse out the relative contributions of indenyl and nitrosyl effects, but the observation that $\Delta S^{\neq}$ values are on the order of -49 eu, while those of (η^5-C_9H_7)Mn(CO)$_3$ are around -26 eu argues for an associative mechanism.

ACKNOWLEDGMENTS

I wish to thank my major professor Thomas E. Bitterwolf for taking me into his lab and being my mentor for the past five years. His encouragements and faith has guided me throughout the research. I would also like to thank my amazing family, my wife Zineb Ali for her highly support, and my daughter Alla, for her helping in writing, my sons Taha, Munieb and Mauwia. None of this work would have been possible without the support, advice, and entertainment provided by my fellow lab mates. I would especially like to thank my government in Libya for financing support. Next, my thanks go out to my committee members and the office staff and other professors at the chemistry department.

Lastly, I would like to thank all my friends that have come and gone over the past years and that have made my time in America the best years of my life.

DEDICATION

This work is dedicated to spirit of my father, Ali Mohamed Altwer

TABLE OF CONTENTS

AUTHORIZATION TO SUBMIT DISSERTATION ii

ABSTRACT……iii

ACKNOWLEDGMENT……..v

DEDICATION……vi

LIST OF FIGURES ……x

LIST OF TABELS ……...xiii

CHAPTER 1 - Introduction 1

1.1 Metal Carbonyls Structure and Bonding 1

1.2 Group VI Metal Carbonyls.....3

1.3 Mechanisms of Metal Carbonyl Substitution Reactions 3

1.4 Indenyl Effect 7

1.5 The Role of Haptotropic Shifts in Some Organometallic Complexes 8

1.6 Indenyl Complex Reactions 12

1.7 Nitrosyl Effects.....13

1.8 Purpose of This Study 16

1.9 Summary 16

1.10 References 17

CHAPTER 2 Synthesis Routes for (η^5-C_9H_7)$M(CO)_2(NO)$ Complexes.....20

2.1 Introduction 20

2.2 Synthesis of (η^5-C_9H_7)$M(CO)_2(NO)$ 21

2.2.1 Experimental.....21

2.2.2 Synthesis of ($\eta^5C_9H_7$)$Cr(CO)_2(NO)$ using NaH route 22

2.2.3 Synthesis of (η^5-C_9H_7)$Cr(CO)_2(NO)$ using sodium metal (Na) and $Cr(CO)_3(CH_3CN)_3$ route 24

2.2.4 Synthesis of (η^5-C_9H_7)$Cr(CO)_2(NO)$ using $Cr(CO)_6$ and n-butyl lithium route 25

2.2.5 Synthesis of (η^5-C_9H_7)$Cr(CO)_2(NO)$ using $Cr(CO)_3(CH_3CN)_3$ and n-BuLi route 26

2.3 Confirmation of (η^5-C_9H_7)$Mo(CO)_3$ Intermediate Formation 27

2.3.1 Synthesis of (η^5-C_9H_7)$Mo(CO)_3(CH_2C_6H_5)$ complex 28

2.4 Results and Discussions 30

2.5 References 31

CHAPTER 3 Study of the Carbonyl Exchange of (η^5-C_9H_7)$Cr(CO)_2(NO)$ with Phosphorus Ligands 32

3.1 Introductions 32

3.2 Experimental Section 33

3.2.1 General procedures 33

3.2.2 Instrumentation 33

3.2.3 Kinetic studies 33

3.3 Kinetics and Mechanism of ligand Substitution in (η^5-C_9H_7)$Cr(CO)_2(NO)$ 36

3.3.1 Kinetics of (η^5-C_9H_7)$Cr(CO)_2(NO)$ thermal decompositions 36

3.3.2 Kinetics of ligand substitution in reaction between (η^5-C_9H_7)$Cr(CO)_2(NO)$ and trimethyphosphine, PMe_3, ligand at 85 to 105 ^oC 40

3.3.3 Study of concentration effects of $P(OMe)_3$ ligand on the reaction rate between the ligand and (η^5-C_9H_7)$Cr(CO)_2(NO)$ complex 46

3.4 References 51

CHAPTER 4 Results and Discussion of the Kinetic Study for the Reaction of $(\eta^5\text{-}C_9H_7)Cr(CO)_2(NO)$ with Phosphorus ligands.....52

4.1 Introduction 52

4.2 Results 52

4.3 Discussions.....54

4.4 Conclusion.....58

4.5 References 59

LIST OF FIGURES

Figure 1-1. Molecular orbital diagram of CO. 1

Figure 1-2. π-back bonding between CO and metal. 2

Figure 1-3. CO bonding modes in metal carbonyl clusters. 3

Figure 1-4. Group VI metal carbonyls. 3

Figure 1-5. Indenyl effect. 7

Figure 1-6. Simplified schematic MO diagram for the $(\eta^5\text{-X})^-$ $[M(CO)_3]^+$ bonding (X= Cp, Ind).[24] 10

Figure 1-7. 3D representation of the $(\eta^5\text{-}C_9H_7)Mn(CO)_3$ LUMO (top) and the $(\eta^5\text{-}C_9H_7)Mn(CO)_2PH_3$ HOMO (bottom).[24] 11

Figure 1-8. [η3+ η2] configuration. 12

Figure 1-9. Electronic structure of NO and it's binding to a metal on ionic and covalent modes.[39] 14

Figure 2-1. IR spectrum of $(\eta^5\text{-}C_9H_7)Cr(CO)_2(NO)$ complex in CH_2Cl_2 23

Figure 2-2. $(\eta^5\text{-}C_9H_7)M(CO)_3$ anion. 28

Figure 3-1. The main steps of kinetic measurements. 35

Figure 3-2. Infrared spectral changes for thermal decomposition of $(\eta^5\text{-}C_9H_7)Cr(CO)_2(NO)$ complex in dodecane at 140 ^oC. 37

Figure 3-3. Plot of natural logarithm of the peak area of the 2023, 1957, and 1711 cm^{-1} bands of the $(\eta^5\text{-}C_9H_7)Cr(CO)_2(NO)$ versus time. Thermal decomposition of $(\eta^5\text{-}C_9H_7)Cr(CO)_2(NO)$ at 150 ^oC in dodecane. 38

Figure 3-4. Plot of natural logarithm of k_{obs} versus (1/T) (activation energy) of thermal decomposition of $(\eta^5\text{-}C_9H_7)Cr(CO)_2(NO)$complex at 140 to 180 ^oC.. 39

Figure 3-5. Infrared spectral changes for the reaction between $(\eta^5\text{-}C_9H_7)Cr(CO)_2(NO)$ (7.1×10^{-5} M) and PMe_3 (5.4×10^{-3} M) In dodecane at 100 ^oC.....40

Figure 3-6. Plot of natural logarithm of peak area of 2023, 1957 and 1711 cm^{-1} bands of $(\eta^5\text{-}C_9H_7)Cr(CO)_2(NO)$ versus time. Reaction takes place between $(\eta^5\text{-}C_9H_7)Cr(CO)_2(NO)$ and PMe_3 in dodcane at 100 ^oC. 42

Figure 3-7. Plot of natural logarithm of (k_{obs}) versus (1/T) (activation energy) of the reaction between $(\eta^5\text{-}C_9H_7)Cr(CO)_2(NO)$ and PMe_3 at 85 to 105 ^oC. 45

Figure 3-8. Plot of natural logarithm of (k/T) versus (1/T) (activation entropy and activation enthalpy) of the reaction between $(\eta^5\text{-}C_9H_7)Cr(CO)_2(NO)$ and $PPhMe_2$ at 95 to 115 ^oC 45

Figure 3-9. Infrared spectral changes for the reaction between $(\eta^5\text{-}C_9H_7)Cr(CO)_2(NO)$ and $P(OMe)_3$ in dodecane at 135 ^oC when the concentration of $P(OMe)_3$ equal 6.4×10^{-4} M.....49

Figure 3-10. Plot of k_{obs} versus $P(OMe)_3$ concentration for the reaction of $(\eta^5\text{-}C_9H_7)Cr(CO)_2(NO)$ with $P(OMe)_3$ in dodecane at 135 ^oC. Concentration of $P(OMe)_3$ changed from (4.0×10^{-4}, 4.8×10^{-4}, 6.4×10^{-4} and 8.0×10^{-4} M) 49

Figure 3-11. Plot of natural logarithm of peak area of 2023, 1957 and 1711 cm^{-1} bands of $(\eta^5\text{-}C_9H_7)Cr(CO)_2(NO)$ versus time. Reaction takes place between $(\eta^5\text{-}C_9H_7)Cr(CO)_2(NO)$ and $P(OMe)_3$ (6.4×10^{-4} M) in dodcane at 135 ^oC. 50

Figure 4-1. Plot of k_{obs} (M^{-1}) versus ligand concentration for the reaction of $(\eta^5\text{-}C_9H_7)Cr(CO)_2(NO)$ with PMe_3, $PPhMe_2$, PBu_3 and $P(OMe)_3$ in dodecane. ...56

Figure 4-2. Plot of kobs versus PR_3 concentration for the reaction of $Mn(\eta^5\text{-}C_9H_7)(CO)_3$ with different PR_3 [PBu_3 and $P(OEt)_3$] concentration in decaline at different temperatures.[3] 57

LIST OF TABLES

Table 1-1. Kinetic data for the $Mn(CO)_5Br$ reaction with phosphine ligands.[11]. 4

Table 1-2. Activation parameters for the reaction of $Ni(CO)_4$ with PPh_3 and CO. 5

Table 3-1. Data for the $k_{(av)}$ for the thermal decomposition of (η^5-C_9H_7)$Cr(CO)_2(NO)$complex versus temperatures. 39

Table 3-2. Data for the $k_{(av)}$ for the reactions of (η^5-C_9H_7)$Cr(CO)_2(NO)$ with PMe_3 ligand at different temperatures in dodecane. Temperature changed from 85 to 105 ^oC. 43

Table 3-3. Data for the $k_{(av)}$ for the reactions of (η^5-C_9H_7)$Cr(CO)_2(NO)$ with $PPhMe_2$ ligand at different temperatures in dodecane. Temperature changed from 95 to 115 ^oC. 43

Table 3-4. Data for the $k_{(av)}$ for the reactions of (η^5-C_9H_7)$Cr(CO)_2(NO)$ with PBu_3 ligand at different temperatures in dodecane. Temperature changed from 125 to 145 ^oC 44

Table 3-5. Data for the $k_{(av)}$ for the reactions of (η^5-C_9H_7)$Cr(CO)_2(NO)$ with $P(OMe)_3$ ligand at different temperatures in dodecane. Temperature changed from 135 to 150 ^oC 44

Table 3-6. Values of enthalpy ($\Delta H^{\ddagger}$) and entropy ($\Delta S^{\ddagger}$) and energy of activation (E_a) for the reaction of (η^5-C_9H_7)$Cr(CO)_2(NO)$ with PMe_3, $PPhMe_2$, PBu_3 and $P(OMe)_3$ in dodecane 46

Table 3-7. Data for the k_{obs} (average) for the reactions of (η^5-C_9H_7)$Cr(CO)_2(NO)$ (7.1×10^{-5} M) with PMe_3 ligand at different PMe_3 concentration at 100 ^oC temperatures.....47

Table 3-8. Data for the k_{obs} (average) for the reactions of $(\eta^5\text{-}C_9H_7)Cr(CO)_2(NO)$ (7.1×10^{-5} M) with $PPhMe_2$ ligand at different $PPhMe_2$ concentration at 100 ^oC temperatures.....47

Table 3-9. Data for the k_{obs} (average) for the reactions of $(\eta^5\text{-}C_9H_7)Cr(CO)_2(NO)$ (7.1×10^{-5} M) with PBu_3 ligand at different PBu_3 concentration at 135 ^oC temperatures.....48

Table 3-10. Data for the k_{obs} for the reactions of $(\eta^5\text{-}C_9H_7)Cr(CO)_2(NO)$ (7.1×10^{-5} M) with $P(OMe)_3$ ligand at different $P(OMe)_3$ concentration at 135 ^oC temperatures.....48

Table 4-1. Infrared carbonyl and nitrosyl absorptions of reaction products in dodecane 53

Table 4-2. The E_B and C_B parameters for phosphines [2].....55

Table 4-3. The cone angle of some phosphines and phosphite ligands.....55

Table 4-4. Basolo rate constants and activation parameters for the substitution reaction of $Mn(\eta^5\text{-}C_9H_7)(CO)_3$ complex with PBu_3 and $P(OEt)_3$ ligands in decalin.....57

Table 4-5. Rate constants and activation parameters for the substitution reaction of $(\eta^5\text{-}C_9H_7)Cr(CO)_2(NO)$ complex with PBu_3 and $P(OMe)_3$ ligands in dodecane....58

CHAPTER 1 Introduction

1.1 Metal Carbonyls Structure and Bonding

Nickel tetra carbonyl $Ni(CO)_4$ the first metal carbonyl, was prepared by A. Mond [1] in 1890 by reaction of metallic nickel with carbon monoxide. Since this discovery, the chemistry of metal carbonyls has been of great interest for several decades, mainly due to structural aspects and their considerable reactivity towards several classes of organic ligands. Metal carbonyls have many applications such as their application in catalysis and as metal organic chemical vapor deposition (OMCVD) precursors in electronic devices. [2-4] Their derivatives are intermediates in homogenous catalytic reactions such as hydrogenation

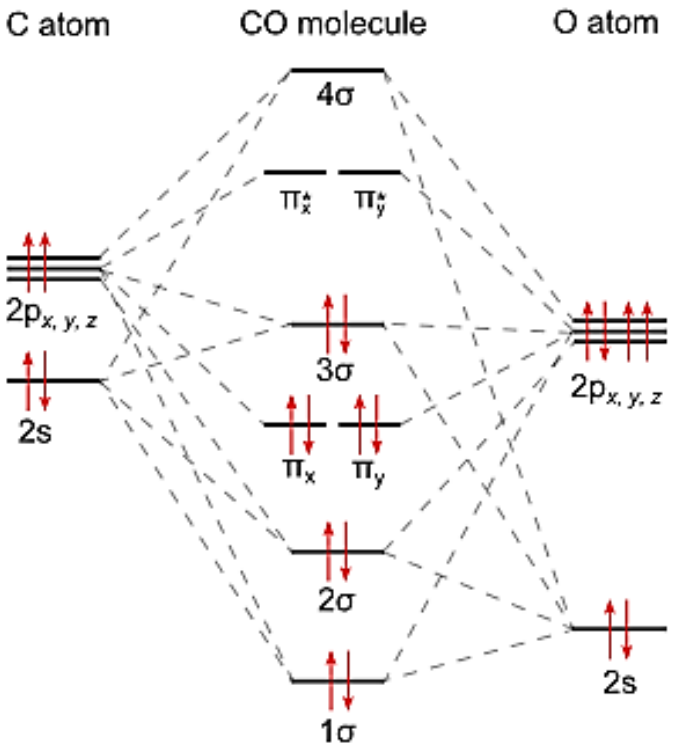

Figure 1-1. Molecular orbital diagram of CO.

and oxygen transfer. They are common starting materials for the synthesis of low-valent metal clusters.[5] The carbonyl ligands in metal carbonyl complexes can be substituted by a large number of ligands such as olefins, arenes and Lewis bases. Carbonyl groups serve as spectroscopic handles in the characterization of metal complexes.[6] In carbonyl compounds, carbon is bonded to oxygen through a triple bond [C≡O]. The molecular orbital picture of CO shows pair of electrons in the 3 σ nonbonding orbital Figure 1-1.

These electrons are available for the "forward" bond in a metal carbonyl bond. IN metal carbonyl a transition metal is bonded to CO. Electron density from the CO 3 σ orbital is donated to the metal forming a sigma bond. The metal atom, in turn, donates electrons from its valence d-orbital to the CO π* orbital making a π back-bond, as seen in Figure 1-2.

CO-M sigma (σ) bond M to CO Pi (π) back bonding.

Figure 1-2. π-back bonding between CO and metal.

Back bonding in to CO antibonding orbitals weakens the C-O bond, as shown by a lengthening of the carbon –oxygen bond and a decrease in the infrared stretching frequencies of the metal bound carbonyl with respect to carbon monoxide. The carbonyl ligand has three common bonding modes in metal carbonyl cluster chemistry.[8] Most commonly, CO binds in the familiar terminal mode, but CO may also bridge between two (μ_2) or three (μ_3) metals, as seen in Figure 1-3.

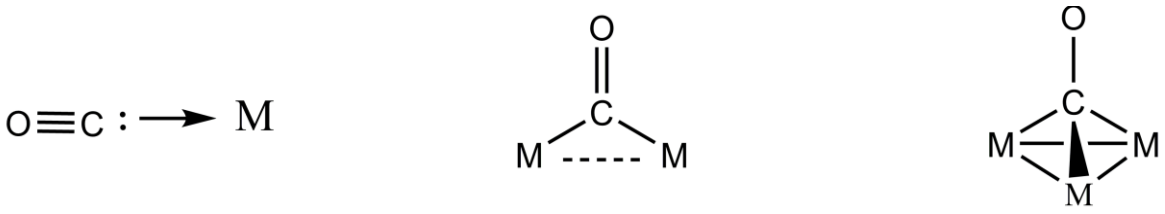

Terminal mode μ_2-bonding mode μ_3 -bonding mode

Figure 1-3. CO bonding modes in metal carbonyl clusters.

1.2 Group VI Metal Carbonyls

The Group (VI) metal carbonyls, $Cr(CO)_6$, $Mo(CO)_6$, $W(CO)_6$ Figure 1-4 are six coordinate 18 e stable compounds with octahedral geometries. In each case the metal has formal oxidation state zero.[9]

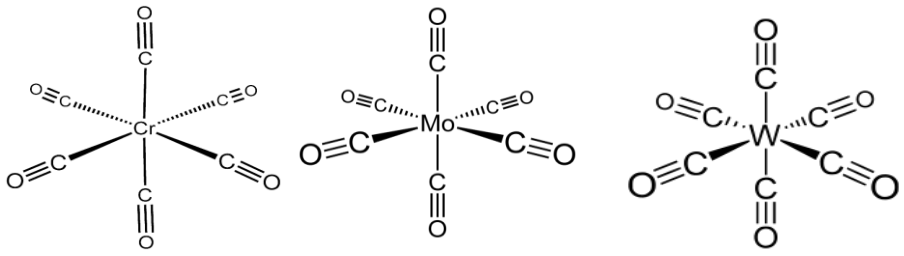

Figure 1-4. Group VI metal carbonyls.

Group VI metal carbonyl are prepared by the reduction of metal halides in the presence of high pressures of carbon monoxide. For example chromium carbonyl can be prepared according to the Equation 1.1:[10]

$$CrCl_3 + Al + 6CO \longrightarrow Cr(CO)_6 + AlCl_3 \qquad (1.1)$$

1.3 Mechanisms of Metal Carbonyl Substitution Reactions

The substitution reactions of metal hexacarbonyl can be represented as follows:

$$M(CO)_n + L \longrightarrow M(CO)_{n-1}L + CO \qquad (1.2)$$

where M is a transition metal and L is an entering ligand. Two examples whose kinetics were investigated by Basolo are shown below.[11, 12]

$$Mn(CO)_5Br + L \longrightarrow Mn(CO)_4LBr + CO \qquad (1.3)$$

$$Ni(CO)_4 + L \longrightarrow Ni(CO)_3L + CO \qquad (1.4)$$

In reaction 1.3, Basolo measured the rate of the substitution reaction of $Mn(CO)_5Br$ by different ligands (PPh_3, $AsPh_3$ and $SbPh_3$) at 30 ^oC in chloroform ($CHCl_3$) solvent. The kinetic data of this reaction shown in Table 1-1 indicate that the rate law is independent of the concentration of ligands, and first order in metal complex.

Table 1-1.

Kinetic data for the $Mn(CO)_5Br$ reaction with phosphine ligands.[11].

ligand	Ligand concentration (M)	Reaction rate [K(10^5 s^{-1})
PPh_3	0.133	6.67
PPh_3	0.344	6.78
$AsPh_3$	0.132	6.56
$AsPh_3$	0.387	6.59
$SbPh_3$	0.135	6.59
$SbPh_3$	0.353	6.65

The second reaction was of $Ni(CO)_4$ with triphenyl phosphine (PPh_3) ligands at different temperatures, using different solvents.

$$Ni(CO)_4 + L \longrightarrow Ni(CO)_3L + CO \qquad (1.5)$$

Where L = PPh_3.

This reaction was also first order behavior in metal complex. And the rate was found to be: rate = k_1 [$Ni(CO)_4$].

The accepted mechanism involves rate-determining step CO dissociation from the 18-electron complex to form a 16-electron intermediate,

$$Ni(CO)_4 \longrightarrow Ni(CO)_3 + CO \quad \text{(slow)} \qquad (1.6)$$

$$Ni(CO)_3 + L \longrightarrow NiCO)_3L \quad \text{(fast)} \qquad (1.7)$$

This substitution reaction is equivalent to an SN_1 reaction in organic chemistry. The values of activation parameters for the two reactions were in agreement with a dissociative process that has a positive entropy ($\Delta S^{\ddagger}$) of activation as shown in Table 1-2.[11-14]

Table 1-2.

Activation parameters for the reaction of $Ni(CO)_4$ with PPh_3 and CO.

ligand	$\Delta H^{\ddagger}$ (Kcal/mol)	$\Delta S^{\ddagger}$ (eu)	K(10^4 s^{-1}) at 20 ^oC
PPh_3	24	13	50
CO	24	14	52

Other studies by Angelici [15] and Brown[16], found that substitution of several metal carbonyl complexes shows a small dependence on the nature and concentration of incoming ligand. Angelici, found that when $Cr(CO)_6$ complex react with different types of ligand such as $AsPh_3$, $P(OPh)_3$, PPh_3, under pseudo first order conditions, the rate law for these substitutions had two terms as shown below for $Cr(CO)_6$ Equation 1.8. Brown arrived at the same conclusion when he reacted the pentacarbonylaminemolybdenum (0) complex,

($Mo(CO)_5A$ (A=amine), with various ligands ($P(OCH_3)_3$, PPh_3, and $AsPh_3$. The second order term was always smaller than the first order term.[15, 16]

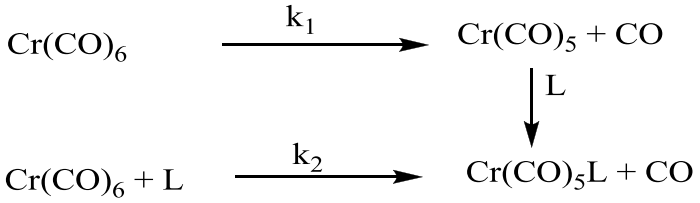

(1.8)

$$\text{Rate} = k_1[Cr(CO)_6] + k_2[Cr(CO)_6][L].$$

Brown has suggested that the second order process follows a dissociative interchange (I_d) mechanism in which a pre-equilibrium forms an associated, weakly bound complex of metal carbonyl and ligand before exchange take place.[16] The interchange model, which has been discussed by Langford and Gray [17] is expressed for the system of interest here by the following Equations:

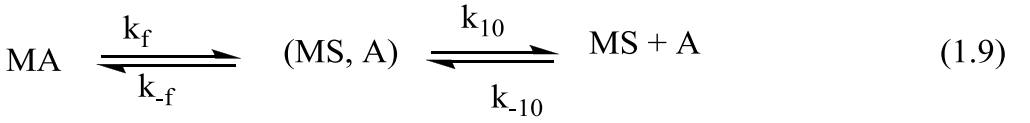

(1.9)

(1.10)

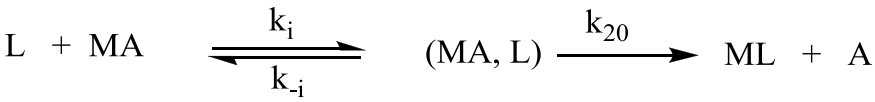

(1.11)

Where S is solvent and the brackets enclose solvent encased substrate and a species occupying a favorable site for exchange. This process seems much more reasonable than the concurrent formation of 16 and 20-electron intermediates that would require in competing dissociative and associative steps. Thus the body of evidence for the simple metal carbonyls

indicates the carbon monoxide dissociation is the most common mechanism of ligand substitution reactions.

1.4 Indenyl Effect

While studying the rates of reaction of $(\eta^5\text{-}C_9H_7)Mo(CO)_3CH_3$ with PR_3 ligands, Hart-Davis and Mawby found that the indenyl complex reacted 20 times faster than the analogous cyclopentadienyl complex.[18] Furthermore, in 1983 Basolo[20] found the indenyl complex of rhodium $(\eta^5\text{-}C_9H_7)Rh(CO)_2$ reacted 3.8 x 10^8 times faster than the cyclopentadienyl complex $(\eta^5\text{-}C_5H_5)Rh(CO)_2$.The enhancement in the rate of associative pathway in the indenyl metal complexes has been termed the "indenyl ligand effect". The indenyl ligand effect arises from particular features of the indenyl ligand as shown in Figure 1-5.

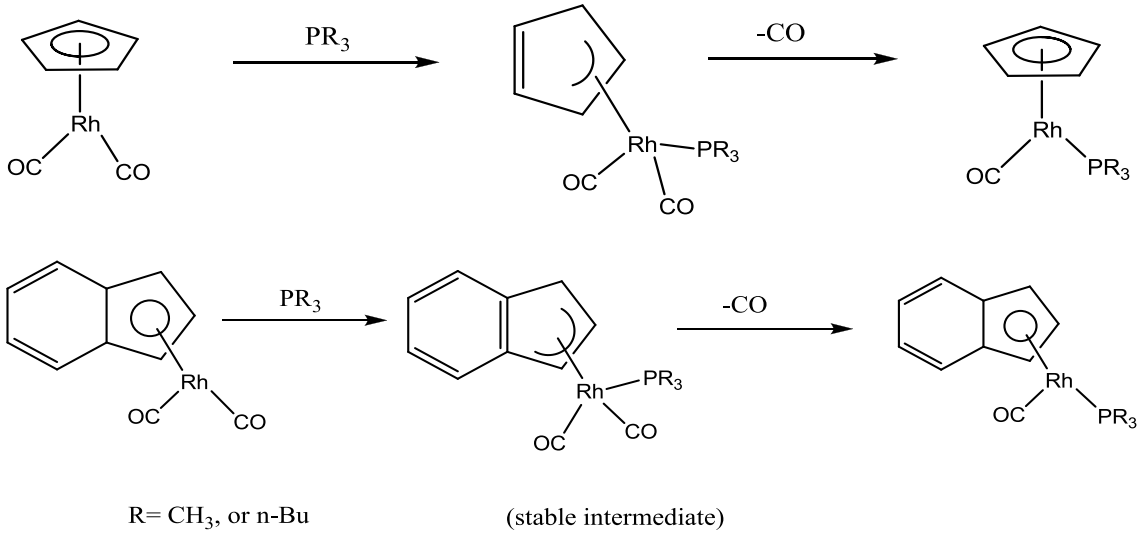

Figure 1-5. Indenyl effect.

In these cases, indenyl 18-electron rhodium complexes undergo associative reactions. In order to maintain an 18 electron count during an associative reaction, the cyclopentadienyl or indenyl ligands must reduce its electron contribution to the metal by two, i.e., go from η^5 to η^3 configuration.[21]. In the case of indenyl complexes, the η^3 intermediate is stabilized by the aromaticity of the benzene ring.[22] The extra stability that comes from aromatic stabilization in the transition state of the indenyl complex cannot take place in the transition state of cyclopentadienyl complex. The aromatic stabilization in the case of indenyl lowers the barrier to formation of an associative intermediate and hence increases the rate of associative pathway of the reaction in the indenyl complexes.

1.5 The Role of Haptotropic Shifts in Some Organometallic Complexes

Hapticity is formally defined as the number of carbon atoms in a ligand that are formally bound to the metal. This definition is relaxed for π bound heteroaromatic ligands to include the hetro atom. Haptotropic changes can occur if new ligands are added to, or removed from the metal. In the current context indenyl and cyclopentadienyl ligands may shift their metal from five carbon to three (η^5-η^3). Indenyl ligands are particularly susceptible to this kind of rearrangement as the η^3 form the ligand retains the aromaticity of the benzene ring. In contrast, cyclopentadienyl rings are far less prone to shift to an η^3 configuration as there is no comparable stabilization. In these cases dissociative reaction pathway are preferred.[22,23] The theoretical understanding of haptotropic shift and bonding in different coordination geometries of polyenic ligands started with pioneer work by Hoffmann et al.[24] More recently, Veiros [25] has done theoretical studies on the addition of PH_3 ligand to (η^5-X)$Mn(CO)_3$ complex where X= cyclopentadienyl (C_5H_5), indenyl (C_9H_7)

and other π ligands. Using B3LYP HF/DFT hybrid functionals. He found that, the addition of a two-electron donor ligand such as PH_3 to an 18-electron complex contain a η^5 coordination π ligands like indene, is expected to induce the η^5 to η^3 haptotropic shift to avoid an unstable 20-electron species. The final coordination geometry of the η^3 ligand results from the balance between electronic factors and van der Waals interligand repulsive and attractive interactions. This is what happens with the solvolysis of $[(\eta^5\text{-}C_9H_7)Mo(CO)_2(MeCN)_2]^+$ in acetonitrile, yielding the structurally characterized $[\eta^3\text{-}C_9H_7)Mo(CO)_2(MeCN)_3]^+$, the process being thoroughly studied by Calhorda.[26] in fact, the two extra electrons added by the incoming PH_3 ligand to the metal center of the manganese complex, $(\eta^5\text{-}X)Mn(CO)_3$ have the same effect; that is, will force the occupation of an X-Mn antibonding orbital, π_{II}^* as shown in Figure 1-6.

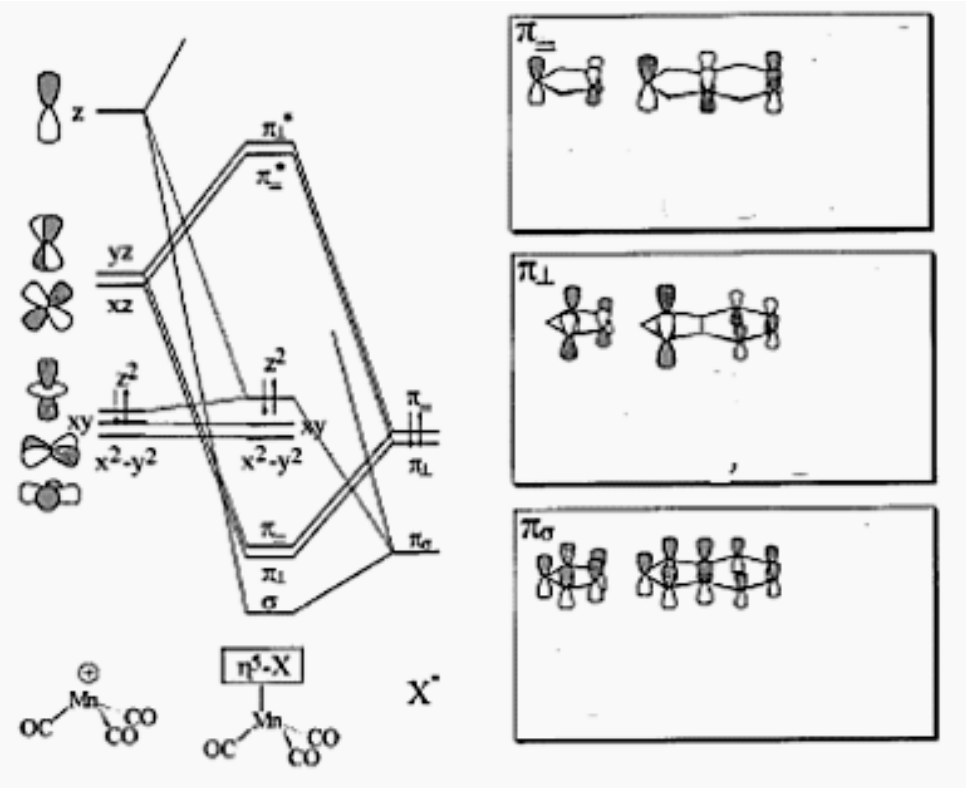

Figure 1-6. Simplified schematic MO diagram for the $(\eta^5\text{-X})^-$ $[M(CO)_3]^+$ bonding (X= Cp, Ind).[24]

The stabilization of this orbital will be the driving force of geometrical distortion associated with the haptotropic shift. This is can be represented when the PH_3 ligand added to $(\eta^5\text{-}C_9H_7)Mn(CO)_3$ complex as shown in Figure 1-7.

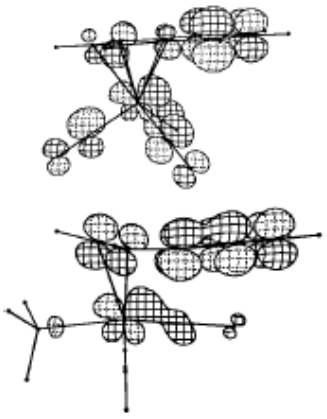

Figure 1-7. 3D representation of the $(\eta^5\text{-}C_9H_7)Mn(CO)_3$ LUMO (top) and the $(\eta^5\text{-}C_9H_7)Mn(CO)_2PH_3$ HOMO (bottom).[24]

The results in the occupation of this complex's lowest unoccupied molecular orbital (LUMO), π_{II}*, which is further stabilized by the indenyl ring folding.

Extended Hückel calculations were performed by Veiros[24] on model complexes $(\eta^5\text{-}C_5H_5)Mn$(polyenyl) based on the optimized geometries with idealized maximum symmetry. This study was done in order to understand the preferred $(\eta^5\text{-}C_5H_5)$ coordination geometry in the phosphine adduct and to compare it with a hypothetical folded cyclopentadienyl complex, $(\eta^5\text{-}C_5H_5)Mn(CO)_3PH_3$. The results showed an η^5 species to be more stable than the η^3 complex by ca 56 k cal/ mol.[26] Finally, Calhorda [27] noted that even with the η^5 coordination with five equivalent M-C bonds are rarely observed for the indenyl ligands. In the most cases the Indenyl ligand is found to coordinate to the metal in a slightly distorted $[\eta^3+ \eta^2]$ configuration. Marder[28] did X ray studies on two $(\eta^5\text{-}C_9H_7)RhL_2$ complexes, L= C_2H_4, PMe_3, and conclude in his study that, the $[\eta^3+ \eta^2]$ configuration was "in between " an η^5 and η^3. In this particular coordinated fashion the bond length between the metal and two carbon atoms C4, C9 is longer than the bond length between the metal

and carbon atoms C1, C2, C3. Marder Also demonstrated that the metal of the indenyl complex is not exactly projected into the pentagonal center of the cyclopentadienyl of the indenyl ring, but it was shifted towards the C1, C2, C3 carbon atoms as shown in Figure 1-8.

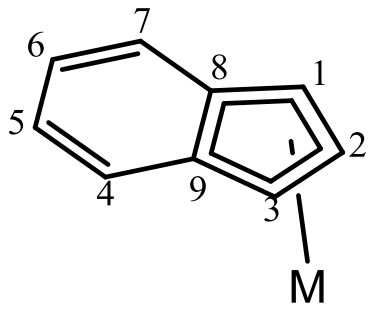

Figure 1-8. [η3+ η2] configuration.

1.6 Indenyl Complex Reactions

The indenyl ligand effect has been found in many classes of organometallic complexes.[29-31] Associative pathways dominate for indenyl complexes relative to cyclopentadienyl complexes.[32] Jones and Mawby and Jones compared the reaction of both $(\eta^5\text{-}C_5H_5)Fe(CO)_2I$ and $(\eta^5\text{-}C_9H_7)Fe(CO)_2I$ with PR_3 ligands. In both reactions carbon monoxide substitution took place by a dissociative SN_1 pathway with the indenyl complex reacting 575 times faster than cyclopentadienyl one.[33] It is worth noting that, the indenyl effect on an associative reaction is shown to be much larger than on a dissociative reaction. This suggest that indenyl stabilizes the transition state for an SN_2 pathway more effectively than it does for an SN_1 path way. The ability of the indenyl ligand to stabilize transition state for SN_2 is due to the electronic nature of the indenyl ligand in the transition state. It has been suggested that indenyl ligand in the excited sixteen electron transition state of the

dissociated intermediate is electron donating towards the metal center with respect to cyclopentadienyl ligand.[34,36] There are many examples indicating not only the rate enhancement in the associative SN_2 pathway but also in the dissociative SN_1 pathway for the indenyl complexes over cyclopentadienyl complexes. Hart-Davis and Mawby compared carbon monoxide substitution by phosphines ligands for $(\eta^5\text{-}C_9H_7)Mo(CO)_3X$ and $(\eta^5\text{-}C_5H_5)Mo(CO)_3X$ complexes (X=Cl, Br, I).[37] Substitution of carbon monoxide in indenyl complexes proceeded by both dissociative SN_1 and associative SN_2 pathways, while analogous cyclopentadienyl complexes proceeded by a dissociative SN_1 mechanism. When the rate constants for the dissociative mechanism were compared in values, the rates of reaction for the indenyl complexes were 6000 times faster than for the cyclopentadienyl complexes.

1.7 Nitrosyl Effects

NO has been found to be important in biological signaling having a biosynthetic pathway and specialized sensor proteins.[38] It forms an extensive series of diamagnetic nitrosyl complexes by binding to odd-electron metal fragments. In the majority of nitrosyl

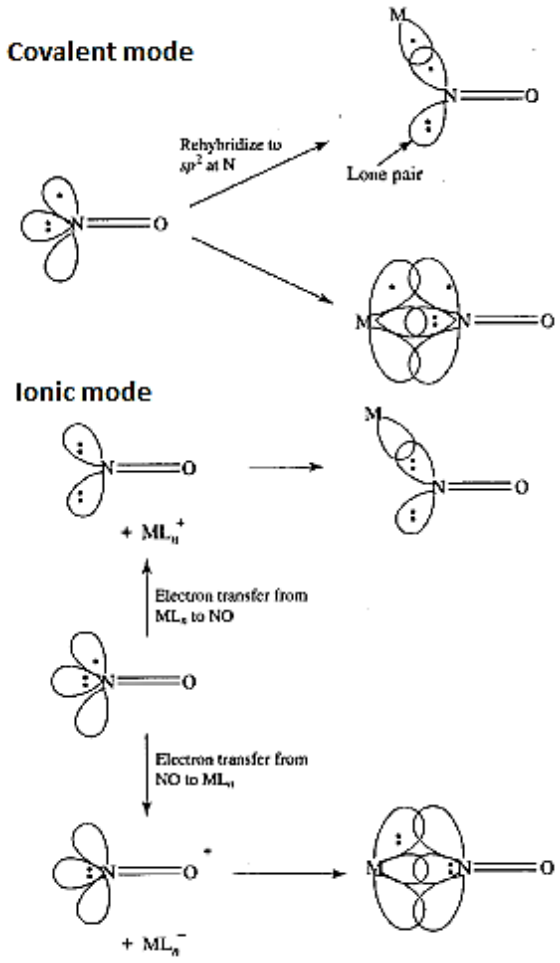

Figure 1-9. Electronic structure of NO and it's binding to a metal on ionic and covalent modes.[39]

complexes, the MNO unit is linear, and such cases, the NO is usually behaving as the 3e donor NO^+ Figure 1-9.[39]

In the covalent model, a linear NO is a 3e ligand. The metal has a singly occupied d_π orbital, which binds with singly occupied NO(π^*) to give an M-N π bond, and the nitrogen (1p) lone pair donates to the empty metal (d_σ) in the normal way to give σ bond. A bent NO is a 1e ligand and the electron occupying a π^* orbital in free NO, the nitrogen atom has to rehybridize to put this electron in an sp^2 orbital pointing toward the metal in order to bind.

Basolo[40] investigated substitution reaction of isoelectronic acid isostructural compounds $Ni(CO)_4$, $Co(CO)_3(NO)$, and $Fe(CO)_2(NO)_2$. He found that $Ni(CO)_4$ reacted by dissociative process, while the nitrosyl carbonyl compounds reacted by associative pathways. This difference was attributed to the ability of the nitrosyl ligand to be bound either as a three electron donating, linear nitrosyl, or in a one electron, bent nitrosyl configuration. As in the case of indenyl, the change in donor behavior of the nitrosyl ligand allows the metal to gain a ligand without exceeding an 18 electron count. This is illustrated bellow.

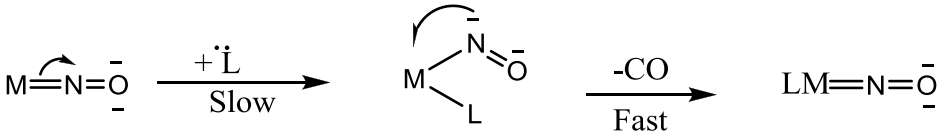

Hall[41] carried out Hartree-Fock- calculations for the ligand substitution of the $W(CO)_4(NO)Cl$ by trimethyl phosphines PMe_3, through the construction of an ab-initio potential energy surface. He predicted an associative mechanism with a 7-coordinate intermediate for the above substitution reaction. The calculated intermediate has a bent nitrosyl ligand with a W-N-O bond angle of 135.70^o. Also, the analysis of charge density distribution of the reaction supports the interpretation that electrons shift to the nitrogen lone pair to vacate a coordinate site for nucleophilic attack. Furthermore, he compared the above reaction with the reaction of $Re(CO)_5Cl$ with PMe_3 and he conclude that, the electronic shifts seen for nitrosyl are not available in the CO substitution of the rhenium compound and substitution of the rhenium species proceeds by a dissociative mechanism.

1.8 Purpose of This Study

This research set out to prepare the series of Group VI compounds, $(\eta^5\text{-}C_9H_7)M(CO)_2(NO)$, by more conventional routes using the reaction of $(\eta^5\text{-}C_9H_7)M(CO)_3$ anions with known NO donors such as Diazald. Subsequent carbonyl exchange kinetics studies were planned with the goal of investigating the indenyl and nitrosyl effects down the Group VI family of compounds.

1.9 Summary

The rate of ligand exchange reaction in indenyl complexes is greater than analogous cyclopentadienyl metal complexes. This behavior is attributed to an indenyl ligand effects.in which the indenyl ligand is able to shift its hapticity from η^5 to η^3 and back. This haptotropic change is stabilized by the recovery of full aromaticity to the benzene ring of the indenyl ligand. Similarly, nitrosyl ligands may shift from a linear, 3e donor, configuration, to a bent, 1e, configuration that also facilitates addition reactions. The family of group VI $(\eta^5\text{-}C_9H_7)Cr(CO)_2(NO)$ complexes may, in principle, exhibit one or both of these behaviors making them attractive targets for kinetics studies.

1.10 References

1) Mond, L.; Langer, C.; Quinck, F. *J. Chem. Soc.* **1890**, 57, 749.
2) Datta, P.; Sinha, C. *Polyhedron*. **2007**, 26, 2433.
3) Ward, M. D. *Coord. Chem. Rev*. **1992**, 115, 1.
4) Casagrand, Jr. O. L.; Tomita, K.; Vollet, D. R. *Polyhedron*. **1996**, 15, 4179.
5) Collman, J. P.; Hegedus, L. S. *Principles and Application of Organotransition Metal Chemistry* (University Science Books, Mill Valley, California, **1980**).
6) Elschenbroich, C.; Salzer, A. *Organometallics*. A. Concise Introduction.VCH Publisher. **1992**.
7) Elschenbroich, C. *Organometallics*. Wiley-VCH. Weinheim. **2006**.
8) Trout, W. E. *J. Chem. Educ*. **1937**, 14, 453-458.
9) Munish, K.; Ayodhya, S. *Eur. J. Chem*. **2012**, 3, 367-394.
10) Huheey, J.; Keiter, E.; Keiter, R. "Metallcarbonyle". *Anorganische Chemie* (2nd ed.). Berlin / New York: de Gruyter. **1995**.
11) Day, J. P.; Basolo, F.; Pearson, R. G.; Kangas, L. F.; Henry, P. M. *J. Am. Chem. Soc.* **1968**, 90, 1925.
12) Angelici, R. J.; Basolo, F. *J. Am. Chem. Soc.* **1962**, 84, 2495.
13) Basolo, F.; Woiciki, A. *J. Am. Chem. Soc*. **1961**, 83, 520.
14) Day, J. P.; Basolo, F.; Pearson, R. G. *J. Am. Chem. Soc*. **1968**, 90, 1925.
15) Graham, J. R.; Angelici, R. J. *Inorg. Chem*. **1967**, 6, 2082.
16) Covey, D. W.; Brown, T. L. *Inorg. Chem*. **1973**, 12, 2820-5.

17) Langford, C. H.; Gray, H. B. "*Ligand Substitution Processes*."W. A. Benjamin, New York, N. Y.; **1965**, Chapter 1.

18) White, C.; Mawby, R.; Hart-Davis, A. *J. Chem. Soc.* (A). **1969**, 2403-2407.

19) Rerek, M.; Liang-Nian, J.; Basolo, F. *J. Chem. Soc. Chem. Comm.* **1983**. 1208.

20) Schuster-Woldan, H.G.; Basolo, F. *J. Am. Chem. Soc*. **1966**, 88, 1657.

21) Casey, C. P.; O'Connor, J .M. *Organometallics*. **1985**, 4, 384.

22) O'Connor. J. M.; Casey, C. P.; *Chem. Rev*. **1987**, 87, 307.

23) Ji, L. N.; Rerek, M. E.; Basolo. F. *Organometallics*. **1984**, 14, 512.

24) Albright, T. A.; Hofmann, P.; Hoffmann, R.; Lillya, C. P.; Dobosh, P. A. *J. Am. Chem. Soc*. **1983**, 105, 3396.

25) Veiros. L. F. *Organometallics*. **2000**, 19, 3127-3136.

26) Calhorda, M. J.; Gamelas, C. A.; Goncalves, I. S.; Herdtweck, E.; Romao, C. C.; Veiros, L. F. *Organometallics*. **1998**, 17, 2597.

27) Calhorda, M. J.; Veiros, L. F. *Coord. Chem. Rev*. **1999**, 37, 185-186.

28) Mareder, T. B..; Calabrese, J. C.; Roe, D.; Tulip, T. H. *Organometallics*. **1987**, 6, 2012.

29) Bitterwolf, T.; Lukmanova, D.; Gallager, S.; Rheingold, A.; Guzei, I.; Liable-Sands, L. *J. Organomet. Chem*. **2000**, 605, 168.

30) Habib, A.; Tanke, R.; Holt, E.; Crabtree, R. *Organometallics*. **1989**, 8, 1225-31.

31) Bang, H.; lynch, T.; Basolo, F. *Organometallics*. **1992**, 11, 40.

32) White, C.; Mawby, R.; Hart-Davis, A. *Inorg. Chim. Acta* **1970**, 4, 441.

33) Jones, D.; Mawby, R. *Inorg. Chim. Acta*. **1972**, 6, 157.

34) Gamasa, P.; Gimeno, J.; Gonzales-Bernardo, C.; Martin-Vaca, B. *Organometallics*. **1996**, 155, 302.

35) White, C.; Mawby, R.; Hart-Davis, A. *Inorg*. *Chim*. *Acta* **1970**, 4, 261.

36) Hodgso, D. J.; Ibers, J. *Inorg*. *Chem*. **1969**, 8, 1282.

37) McCleverty, J. A. *Chem*. *Rev*. **2004**, 104, 403.

38) Faller, J. W. *J*. *Organomet*. *Chem*. **1990**, 383, 161.

39) Crabtree, R. H. (**2005**). *The Organometallic Chemistry of the Transition Metals*. (4th ed.). Hoboken, New Jersey: Jhon Wiley & Sons.

40) Thorsteinson, E. M.; Basolo, F. *J*. *Am*. *Chem*. *Soc*. **1969**, 8, 3200.

41) Song, J.; Hall. M. B.; *J*. *Am*. *Chem*. *Soc*. **1993**, 115, 327-336.

CHAPTER 2 Synthesis Routes for $(\eta^5\text{-}C_9H_7)M(CO)_2(NO)$ Complexes

2.1 Introduction

The reactivity of the cyclopentadienyl compounds is changed when cyclopentadienyl rings is replaced with indenyl as a result of the kinetic indenyl effect.[1] the synthesis of the Group VI cyclopentadienyl, carbonyl compounds were first reported in 1954 by Wilkinson who prepared $[(\eta^5\text{-}C_5H_5)M(CO)_3]_2$, where (M= M_O and W) using a high temperature reaction of the metal carbonyl with cyclopentadiene vapor.[2] in 1955, Fischer[3] reacted $(\eta^5\text{-}C_5H_5)_2Cr$ with CO under high pressure to produce $[(\eta^5\text{-}C_5H_5)Cr(CO)_3]_2$. Shortly thereafter it was found that the family of compounds, $[(\eta^5\text{-}C_5H_5)M(CO)_3]_2$ could be more conveniently prepared by reaction of $M(CO)_6$ with an alkali metal cyclopentadienide.[4] Scheme 2-1 shows the Wilkinson synthesis of the $(\eta^5\text{-}C_5H_5)M(CO)_2(NO)$ (M= Cr, Mo, W).[5]

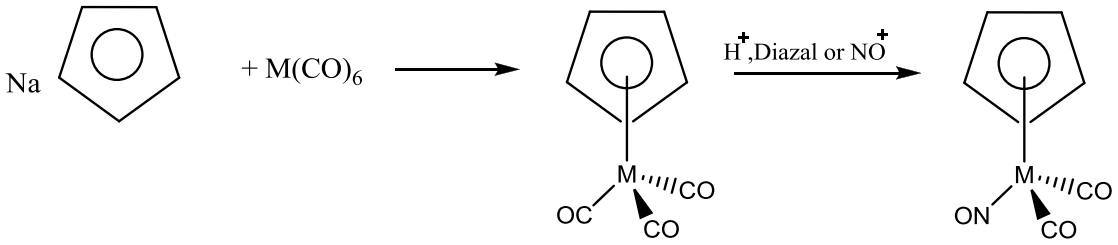

M= Cr, Mo, W

Scheme 2-1. Synthesis of $(\eta^5\text{-}C_5H_5)M(CO)_2(NO)$ complexes.

The $(\eta^5\text{-}C_9H_7)Mo(CO)_3$ dimer was reported by King and Stone[6] and later improved upon by King and Binsette.[7] The tungsten dimer was reported by Nesmeyanov, et al.[8] the corresponding chromium dimer is unknown, possibly because of facile Cr-Cr bond breaking. Reduction of the Mo or W dimers with sodium yields the anion $(\eta^5\text{-}C_9H_7)M(CO)_3^{-1}$, that can undergo reaction with alkyl halides to yield $(\eta^5\text{-}C_9H_7)M(CO)_3$ R, Ultimately, the anions $(\eta^5\text{-}C_9H_7)M(CO)_3^{-1}$, may be prepared by formation of the indenyl anion followed by reaction with $M(CO)_6$ or one several more reactive intermediates including $M(CO)_3(NCMe)_3$, $M(CO)_3Py_3$ or $M(CO)_3(NH_3)_3$. Even under ideal conditions the yields of the anion are difficult to reproduce and are often low. Although the $(\eta^5\text{-}C_5H_5)M(CO)_2(NO)$ derivatives for Cr, Mo and W are known, the, only $(\eta^5\text{-}C_9H_7)Cr(CO)_2(NO)$ complex was reported in 1976 by Herberhold[9] . The compound was prepared using $CrCl(CO)_2(NO)Py_2$ as precursor. This paper appears to be the only mention of the chromium precursor in the literature and no comparable complex of Mo or W has been reported. We were interested in finding an alternative route to the chromium compound and routs to the molybdenum and tungsten derivatives. We wished to do kinetics studies of $(\eta^5\text{-}C_9H_7)M(CO)_2(NO)$ as these compounds might be expected to exhibit both indenyl and nitrosyl effect.

2.2 Synthesis of $(\eta^5\text{-}C_9H_7)M(CO)_2(NO)$

2.2.1 Experimental

All reactions were carried out under nitrogen using standard Schlenk techniques. Tetrahydrofuran (THF) was distilled under nitrogen prior to use. Indene was purchased from Acros, and was distilled prior to use. Sodium hydride was purchased from Aldrich and used as received. Diazald was purchased from Aldrich. Group VI hexacarbonyl compounds,

$Cr(CO)_6$, $Mo(CO)_6$, and $W(CO)_6$ were purchased from Strem Chemicals. Tris (acetonitrile) chromium carbonyl $Cr(CO)_3(CH_3CN)_3$ was prepared according to literature method.[10] Infrared spectra were recorded on a Perkin-Elmer Spectrum 1000 FT-IR. Nuclear magnetic resonance (NMR) spectra were recorded using a Bruker AMX 300 spectrometer using $CDCl_3$ as solvent.

2.2.2 Synthesis of ($\eta^5C_9H_7$)$Cr(CO)_2(NO)$ using NaH route

Sodium hydride (0.24 g 10 mmol) was added to 25 mL of THF containing indene (2.3 ml) and the mixture was refluxed for 2 hours. At this point chromium hexacarbonyl, $Cr(CO)_6$, (2.2 g, 10 mmol) was added. The reaction mixture was refluxed for 4 days, at which time the IR spectrum indicated that the reaction was completed by disappearance of the starting material absorption signal at 2023, 1957, and 1711 cm^{-1} Diazald (2.2 g, 10 mmol) was added at room temperature and the reaction was stirred for 30 minutes. The solvent was removed yielding a dark brown precipitate. The precipitate dissolved in dichloromethane and the solution filtered to remove solids. The dark red solution was concentrated before chromatography on silica gel. Elution was carried out by mixture of dichloromethane and petroleum ether (1:10 ratio). The orange band was collected under nitrogen and the solvent was removed to yield dark orange oil (η^5-C_9H_7)$Cr(CO)_2(NO)$ in 18% yield as shown in Scheme 2-2. The product was characterized by Infrared spectroscopy as shown in Figure 2-1. IR (CH_2Cl_2): 2023, 1957, 1711.cm^{-1} in contrast with IR spectra data reported by Herberhold[9] IR (C_6H_6): 2019, 1946, 1699 cm^{-1}. ^1H NMR ($CDCl_3$): δ = 7.44-7.40 (m, 2H, C_9H_7), 7.25-7.22 (m, 2H, C_9H_7). 5.9 (s, 2H, C_9H_7), 5.65(s, 1H, C_9H_7).

^{13}C NMR ($CDCL_3$): δ = 237.08 (CO), 126.3, 124.8 (C_9H_7), 110.2 (C_9H_7), 95.4 (C_9H_7), 79.4 (C_9H_7) ppm.

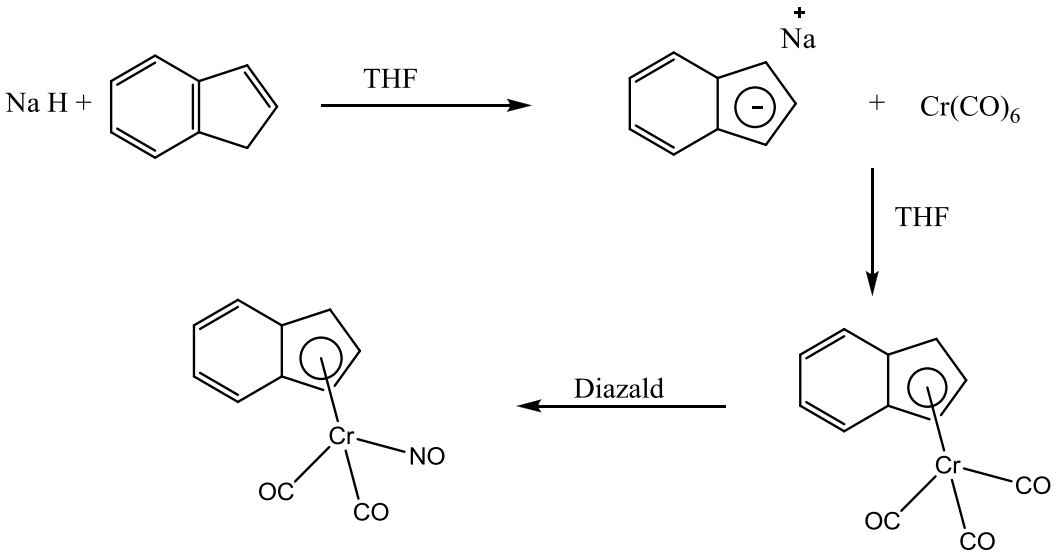

Scheme 2-2. Synthesis of $(\eta^5\text{-}C_9H_7)Cr(CO)_2(NO)$ using NaH route.

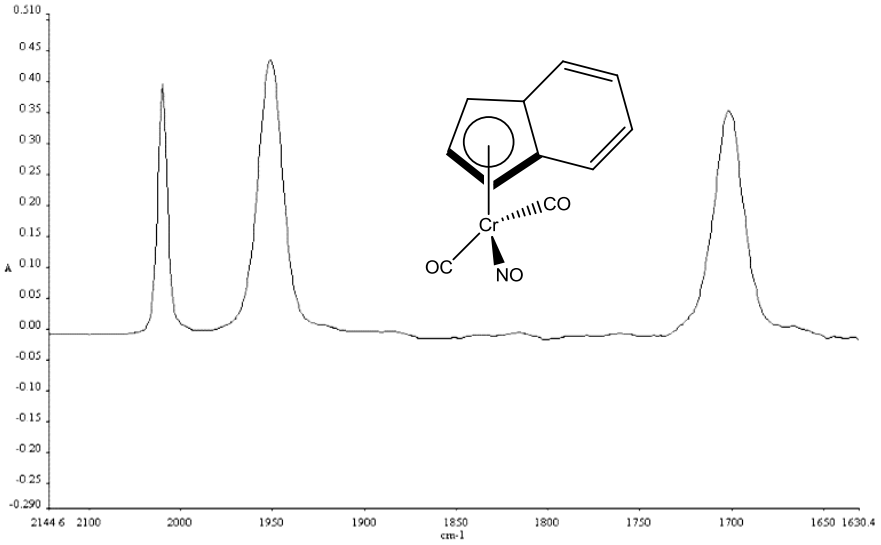

Figure 2-1. IR spectrum of $(\eta^5\text{-}C_9H_7)Cr(CO)_2(NO)$ complex in CH_2Cl_2 .

2.2.3 Synthesis of $(\eta^5\text{-}C_9H_7)Cr(CO)_2(NO)$ using sodium metal (Na) and $Cr(CO)_3(CH_3CN)_3$ route

Sodium metal (0.23 g, 10 mmol) was added to 25 mL of THF and then indene 2.3 ml was added and refluxed for 2 hours. Tris(acetonitrile)chromiumtricarbonyl, $Cr(CO)_3(CH_3CN)_3$ prepared from 2.2 g of $Cr(CO)_6$ in refluxing acetonitrile was added. The reaction mixture was refluxed for 2 days, at which time the IR spectrum indicated that the reaction was completed by disappearance of the starting martial absorption signal. The Diazald (2.2 g, 10 mmol) was added at room temperature and the reaction stirred for 30 minutes. The solvent was removed leaving dark brown precipitate that was purified by chromatography as described above. The orange band was collected under nitrogen and the solvent was removed to yield dark red oil $(\eta^5\text{-}C_9H_7)Cr(CO)_2(NO)$ in 20% yield as shown in Scheme 2-3.

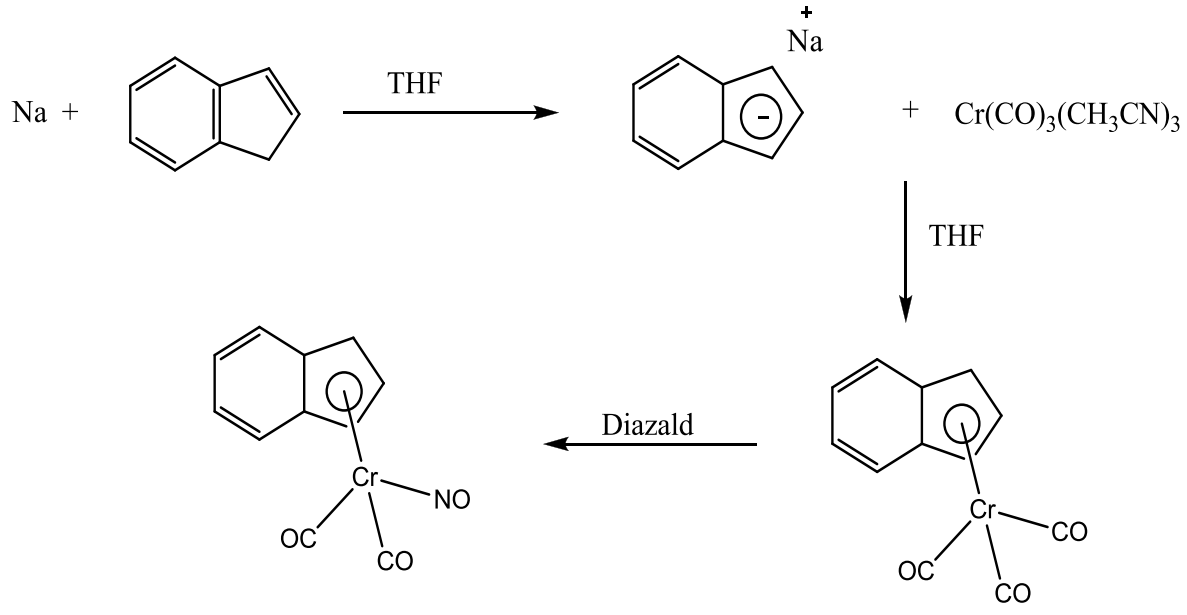

Scheme 2-3. Synthesis of $(\eta^5\text{-}C_9H_7)Cr(CO)_2(NO)$ using Na metal and acetonitrile route.

2.2.4 Synthesis of $(\eta^5\text{-}C_9H_7)Cr(CO)_2(NO)$ using $Cr(CO)_6$ and n-butyl lithium route

In a Schlenk flask under inert atmosphere a solution of freshly distilled indene (1 ml, 8.6 mmol) in 30 ml THF was cooled to 0 ^oC, and n-BuLi (1.2 M solution in hexane, 4.5 ml, 8.8 mmol) was added. The light orange solution of LiC_9H_7 was stirred for 30 min and allowed to warm to room temperature. $Cr(CO)_6$ (1.43 g, 6.5 mmol) was added and the mixture refluxed for 24 h. A brown solution was obtained, which was cooled to room temperature. Diazald (2.2 g, 10 mmol) was added and, after stirring for 30 minutes, the solvent was removed to give a dark brown precipitate. And was purified by chromatography as described above. An orange band was collected under nitrogen and the solvent was removed to yield dark orange oil $(\eta^5\text{-}C_9H_7)Cr(CO)_2(NO)$ in 27% yield as shown in. Scheme 2-4.

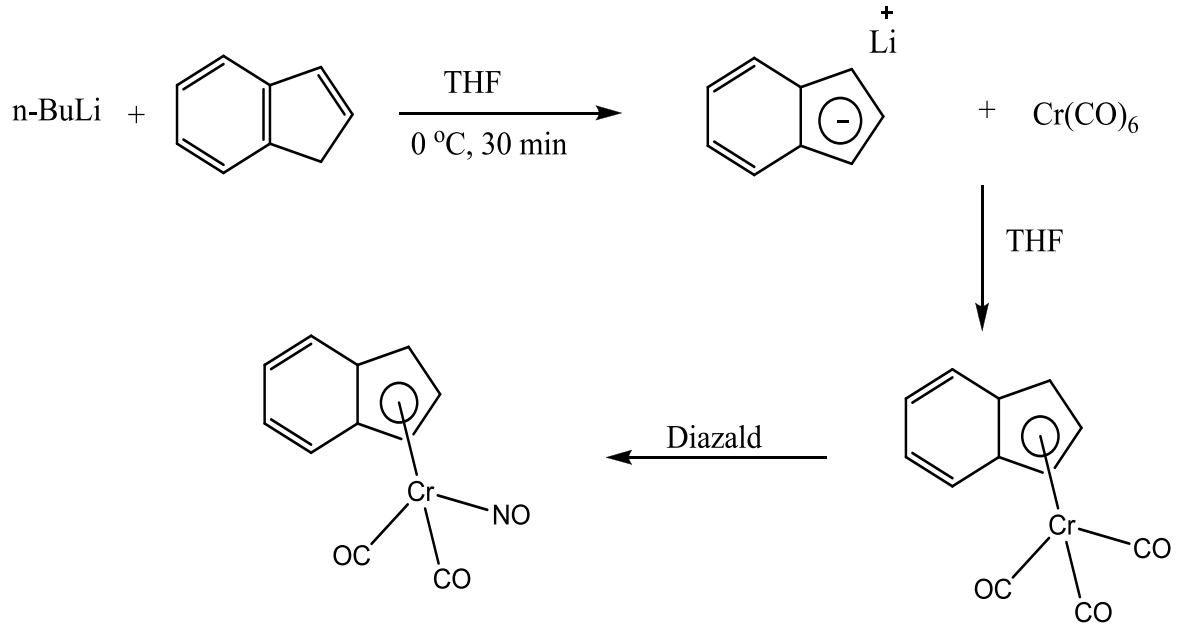

Scheme 2-4. Synthesis of $(\eta^5\text{-}C_9H_7)Cr(CO)_2(NO)$ using n-BuLi route.

2.2.5 Synthesis of $(\eta^5\text{-}C_9H_7)Cr(CO)_2(NO)$ using $Cr(CO)_3(CH_3CN)_3$ and n-BuLi route

In a Schlenk flask under inert atmosphere a solution of freshly indene (1 ml, 8.6 mmol) in 30 ml THF was cooled to 0 ^oC, and n-BuLi (1.2 M solution in hexane, 4.5 ml, 8.8 mmol) was added. The light orange solution of LiC_9H_7 was stirred for 30 min and allowed to warm to room temperature. $Cr(CO)_3)(CH_3CN)_3$ prepared from 2.2 g of $Cr(CO)_6$ in refluxing acetonitrile was added and the mixture refluxed for 24 h. A brown solution was obtained, which was cooled to room temperature. Diazald (2.2 g, 10 mmol) was added and, after stirring for 30 minutes, the solvent was removed and dark brown precipitate was formed and was purified by chromatography as described above. An orange band was collected under nitrogen and the solvent was removed to yield a dark orange oil $(\eta^5\text{-}C_9H_7)Cr(CO)_2(NO)$ in 52% yield as shown in Scheme 2-5.

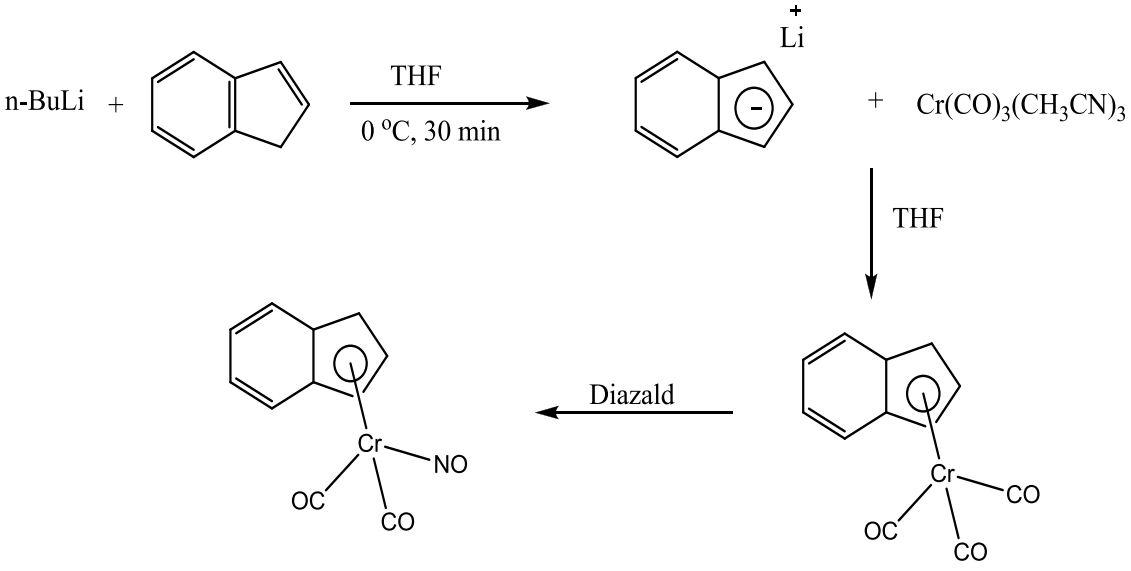

Scheme 2-5. Synthesis of $(\eta^5\text{-}C_9H_7)Cr(CO)_2(NO)$ using n-BuLi and $Cr(CO)_3(CH_3CN)_3$ route.

Attempted synthesis of $(\eta^5\text{-}C_9H_7)M(CO)_2(NO)$, where M = Mo, and W. The family of Group VI $(\eta^5\text{-}C_5H_5)M(CO)_2(NO)$ derivatives is well known and can be prepared by reaction of the corresponding $(\eta^5\text{-}C_5H_5)M(CO)_3$ anion with Diazald or other NO sources. In our hands, reaction of the $(\eta^5\text{-}C_9H_7)M(CO)_3$ anions with several NO transfer agents including Diazald, tritylthionitrosyl, and n- butylnitrite resulted in the formation of the corresponding $[(\eta^5\text{-}C_9H_7)(CO)_3]$ dimers based on the infrared spectrum[6] with no evidence of the desired nitrosyl derivatives. Our failure to isolate the corresponding indenyl derivatives prompted an investigation into formation, and reactivity, of $(\eta^5\text{-}C_9H_7)M(CO)_3$ anions. King and Bisnette[6] prepared the $(\eta^5\text{-}C_9H_7)M(CO)_3$ anion by sodium reduction of the M-M bonded $[(\eta^5\text{-}C_9H_7)M(CO)_3]_2$ dimer. Reaction of these anions with MeI yielded $(\eta^5\text{-}C_9H_7)M(CO)_3Me$. As we were preparing the intermediate anions by direct reaction of LiC_9H_7 with $M(CO)_6$ or $M(CO)_3(NCCH_3)_3$ we decided to test our intermediates that showed IR at by reaction with benzyl bromide.

2.3 Confirmation of $(\eta^5\text{-}C_9H_7)Mo(CO)_3$ Intermediate Formation

Although, the synthesis of nitrosyl derivative of molybdenum and tungsten was not successful, the formation of anion intermediate of Mo as seen in Figure 2-2, was confirmed by reaction this intermediate with benzylbromide. The resulting benzyl-complex was isolated and characterized by both IR and NMR spectroscopy methods. (Section 2.3.1).

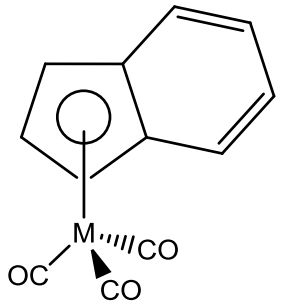

Figure 2-2. $(\eta^5\text{-}C_9H_7)M(CO)_3$ anion.

2.3.1 Synthesis of $(\eta^5\text{-}C_9H_7)Mo(CO)_3(CH_2C_6H_5)$ complex

All reactions were carried out under nitrogen using standard Schlenk techniques. Tetrahydrofuran (THF) was distilled under nitrogen prior to use. Indene was purchased from Acros also distilled prior to use. N-butyllithium was purchased from Alfa Aesar. Molybdenum hexacarbonyl $Mo(CO)_6$, was purchased from Strem Chemicals. Benzyl bromide ($C_6H_5CH_2Br$) was purchased from Alfa Aesar. Infrared spectra were recorded on Perkin-Elmer Spectrum 1000 FT-IR spectrometer. Nuclear magnetic resonance (NMR) spectra were recorded using a Bruker AMX 300 spectrometer.

In a Schlenk flask under inert atmosphere a solution of indene (1 ml, 8.6 mmol) in THF (40 ml) was cooled to 0 ^oC, and n-BuLi (1.2 M solution in hexane, 4.5 ml, 8.8 mmol) was added. The light orange solution of LiC_9H_7 was stirred for 30 min and allowed to warm to room temperature. Molybdenum hexacarbonyl, $Mo(CO)_6$, (1.7 g, 5.5 mmol) was added and the mixture refluxed for 24 h. A brown solution was obtained, which cooled to room temperature. Benzyl bromide ($C_6H_5CH_2Br$, 1.2 ml, 7 mmol) was added and was stirred overnight; the solvent was removed under reduced pressure to give a brown residue. This

residue was purified by dry column chromatography under inert atmosphere. The target compound was eluted as an orange band with mixture of petroleum-ether and dichloromethane. Evaporation of the solvents afforded an orange solid of $(\eta^5\text{-}C_9H_7)Mo(CO)_3(CH_2C_6H_5)$. Yield: 0.39 g, 19.5 %. As shown in Scheme 2-6. IR (CH_2Cl_2): 2013, 1930 cm^{-1} as shown in Figure 2

^{1}H NMR ($CDCl_3$): δ = 7.30-7.34 (m, 2H, C_9H_7), 7.24-7.28 (m, 2H, C_9H_7) 7.03-7.11 (m, 4H, Ph), 6.93-6.98 (m, 1H, Ph), 5.8 (d, 2H, C_9H_7), 5.37-5.39 (t, 1H, C_9H_7), 1.66 (s, 2H, -CH_2) ppm.^{13}CNMR ($CDCL_3$): δ = 240.0 (CO trans to –CH2-Ph), 228.2 (CO cis to –CH2-Ph), 127.8, 126.6 (C_9H_7), 112.8 (C_9H_7), 124.7, 124.0 (C ph), 148.6 (C ph), 91.4 (C_9H_7), 81.0 (C_9H_7), 17.3 (CH_2).ppm.

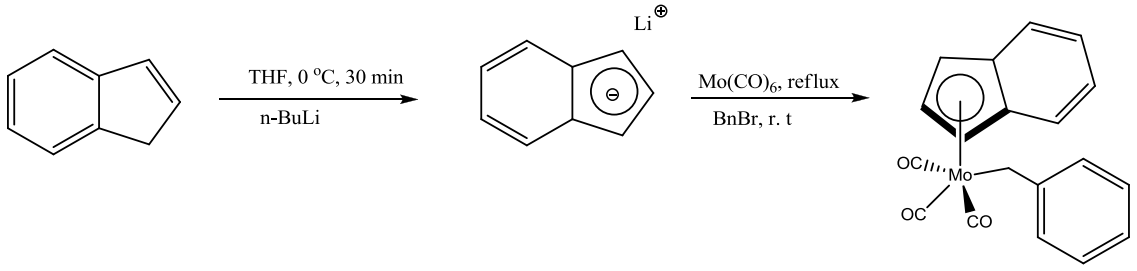

Scheme 2-6. Synthesis of $(\eta^5\text{-}C_9H_7)Mo(CO)_3(CH_2C_6H_5)$ complex.

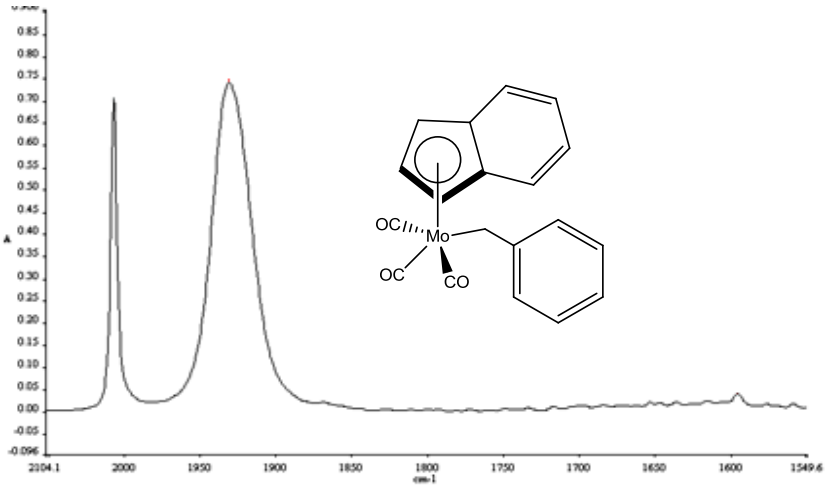

Figure 2-3. Infrared spectra of $(\eta^5\text{-}C_9H_7)Mo(CO)_3(CH_2C_6H_5)$ complex.

2.4 Results and Discussions

Several routes to the synthesis of $(\eta^5\text{-}C_9H_7)Cr(CO)_2(NO)$ were investigated. Optimal yields were achieved by preparing the intermediate anion by reaction of LiC_9H_7 with $Cr(CO)_3(NCCH_3)_3$ followed by reaction of the anion with Diazald. Attempts to extend these synthesis to $(\eta^5\text{-}C_9H_7)M(CO)_2(NO)$, where M= Mo and W were unsuccessful. Reaction of the $(\eta^5\text{-}C_9H_7)M(CO)_3$ anions with benzylbromide cleanly yielded the corresponding $(\eta^5\text{-}C_9H_7)Mo(CO)_3(CH_2C_6H_5)$ complex in good yield. As the corresponding $(\eta^5\text{-}C_5H_5)M(CO)_2(NO)$ derivatives are known, the failure to isolate the Mo, and W analogues is puzzling.

2.5 References

1) Rerek, M.; Liang-Nian, J.; Basolo, F. *J. Chem. Soc. Comm.* **1983**, 1208.
2) Wilkinson, G. *J. Am. Chem. Soc.* **1954**, 76, 209-211.
3) Fischer, E. O.; Hafner, W. *Z. Naturforsch.* **1955**, 10b, 140-3.
4) Fischer, E. O.; Hafner, W.; Stahl, H. O. *Z. Anorg. Allege. Chem.* **1955**, 282, 47-62.
5) Piper, T. S.; Wilkinson, G. *J. Inorg. Nuc. Chem.* **1956**, 3, 104.
6) King, R. B.; Stone, F. G. A. *J. Am. Chem. Soc.* **1960**, 82, 4557-4562.
7) King, R. B.; Bisnette, M. B. *Inorg. Chem.* **1965**, 4, 475-81.
8) Nesmeyanov, A. N.; Ustynyuk, N. A.; Makarova, L. G.; Andrianov, V. G.; Struchkov, Yu. T.; Andrae, S.; Ustynyuk, Yu. A.; Malyugina, S. G. *J. Oranomet. Chem.* **1978**, 159, 189-99.
9) Herberhold, M.; Bernhasen, W. *Angew. Chem.* **1976**, 15, 617.
10) Dobson, G, R.; Amr El Sayed, M, F.; Stolz, I. W.; Sheline, R. K. *Inorg. Chem.* **1962**, 1, 526-30

CHAPTER 3 Study of the Carbonyl Exchange of $(\eta^5\text{-}C_9H_7)Cr(CO)_2(NO)$ with Phosphorus Ligands

3.1 Introductions

As described in Chapter 1 indenyl, and nitrosyl transition metal complexes undergo ligand exchange at faster rates than their cyclopentadienyl, or carbonyl analogs. In this chapter $(\eta^5\text{-}C_9H_7)Cr(CO)_2(NO)$ will be shown to exhibit rate enhancement. Burnner[1] attempted to react the $(\eta^5\text{-}C_5H_5)Cr(CO)_2(NO)$ with PPh_3 under thermal conditions. He reported that in refluxing toluene, bp 110 ^oC over extended periods there was no reaction, and in refluxing decane, bp 174 ^oC, the chromium complex decomposed to give a chromium mirror. The monosubstituted product was obtained by heating in molten PPh_3 at 160 ^oC. The reaction was slow and gave many side-products. Despite this sluggish reactivity, Brunner noted that $(C_5H_5)Cr(CO)_2(NO)$ was more reactive than $(C_5H_5)Mn(CO)_3$ which is inert in molten PPh_3. "More reactive" in this case is stretching it as molten ligand is not a "normal" reaction condition. Casey[2] studied the reaction of $(\eta^5\text{-}C_5H_5)M(CO)_2(NO)$, where M= Mo and W with trimethyl phosphine PMe_3 and found the reaction to proceed rapidly in THF at 25 ^oC to give $(\eta^5\text{-}C_5H_5)M(CO)(NO)(PMe_3)$ rates of 2.71 x 10-1 M^{-1} sec^{-1} and 4.48 x 10 $^{-2}$ M^{-1} sec^{-1} respectively. Reaction of $(\eta^5\text{-}C_5H_5)W(CO)_2(NO)$ with PPh_3 is reported to be much slower than with PMe_3, raising the interesting question of whether $(\eta^5\text{-}C_9H_7)M(CO)_2(NO)$ might also react more rapidly with PMe_3 than PPh_3 To our knowledge there are no kinetic studies of Group VI complexes $(\eta^5\text{-}C_9H_7)M(CO)_2(NO)$, where M = Cr, Mo ,W with PR_3 ligands. Therefore, in this chapter we present out studies of reaction of the $(\eta^5\text{-}C_9H_7)Cr(CO)_2(NO)$

complex with PR_3 ligands (PMe_3, $PPhMe_2$, PBu_3 and $P(OMe)_3$ to understand its mechanism and possible contributions of both indenyl and nitrosyl ligands effects reactivity.

3.2 Experimental Section

3.2.1 General procedures

The $(\eta^5\text{-}C_9H_7)Cr(CO)_2(NO)$ complex used in this work is air and moisture sensitive. All manipulations were carried out under an atmosphere of N_2, using standard Schlenk techniques or in a N_2-filled glove box. Dodecane was used as a solvent and was sparged with N_2 for at least one hour prior to use.

3.2.2 Instrumentation

Infrared spectra were obtained on a Perkin-Elmer Spectrum 1000 FT-IR spectrometer using a 0.5-mm path length NaCl cell. A special high temperature bath and the main steps of the experiments were constructed as shown in Figure 3-1.

3.2.3 Kinetic studies

All kinetic experiments were run under pseudo-first-order conditions (at least a 10-fold excess of phosphines, PR_3). The ligand solution (3 mL) and 1.5 ml of a chromium complex solution were equilibrated side-by-side in a constant temperature bath. After stabilization of the temperature, the metal complex solution was rapidly transferred into the ligand solution by cannula transfer. This method permitted the transfer to take place without cooling of the solution. The solution of the metal complex was prepared by dissolving 0.018 g of $(\eta^5\text{-}C_9H_7)Cr(CO)_2(NO)$ in 1.5 ml of dodecane. The reaction rate was monitored

by the decrease of the chromium complex bands at 2023, 1957, and 1711 cm^{-1}. Samples for analysis were obtained by withdrawing ~ 0.3 mL aliquots of the reaction mixture and transferring these samples to an IR cell. The difference in temperature between the reaction bath and sampling syringe was sufficient to quench the reaction.

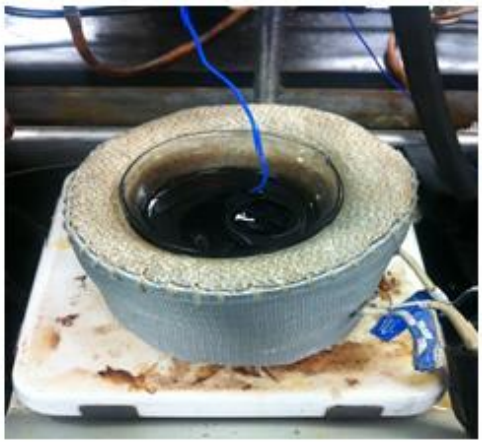

(a) Special Temperature bath.

(b) Temperature controller.

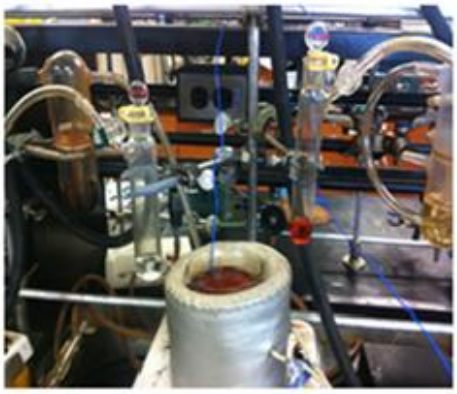

(c) preparation of ligand and Cr complex mixture.

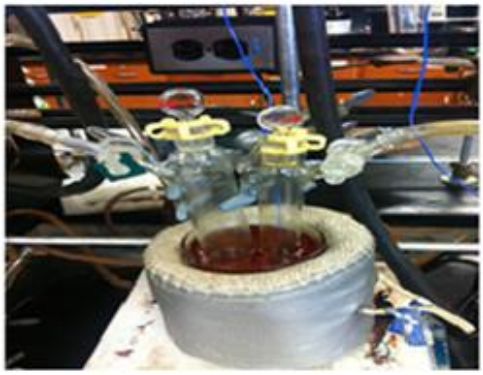

(d) Ligand and Cr complex solutions were equilibrated in constsnt temperature

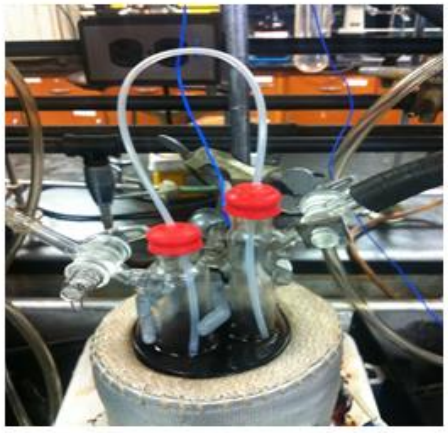

(e) Cannula transfer mixing the ligand and complex soluation.

Figure 3-1. The main steps of kinetic measurements.

3.3 Kinetics and Mechanism of ligand Substitution in (η^5-C_9H_7)$Cr(CO)_2(NO)$

3.3.1 Kinetics of (η^5-C_9H_7)$Cr(CO)_2(NO)$ thermal decompositions

Prior to the kinetics study of the ligand substitution for the indenyl complex, we examined the thermal decomposition of the complex at three different temperatures (140, 150, and 180 ^oC) in order to calculate the rate of decomposition of the complex. Recording the kinetics at multiple temperatures makes it possible to extract thermodynamics data for comparison with the ligand exchange values. The rate of the decomposition was monitored by infrared spectroscopy. Figure 3-2 shows the spectrum over time of disappearance of the starting material bands 2023, 1957 and 1711 cm^{-1} at 140 ^oC. Figure 3-3 shows the values of the rate constant, k for each run. The rate constant values were obtained from slopes of a plot of the natural logarithm of the peak area, ln[A], of the two carbonyl and nitrosyl vibration bands versus time. For each temperature at least three kinetic runs were recorded. The rate constants presented in Table 3-1 are the arithmetic average of rate constants from three kinetics runs under the same conditions.

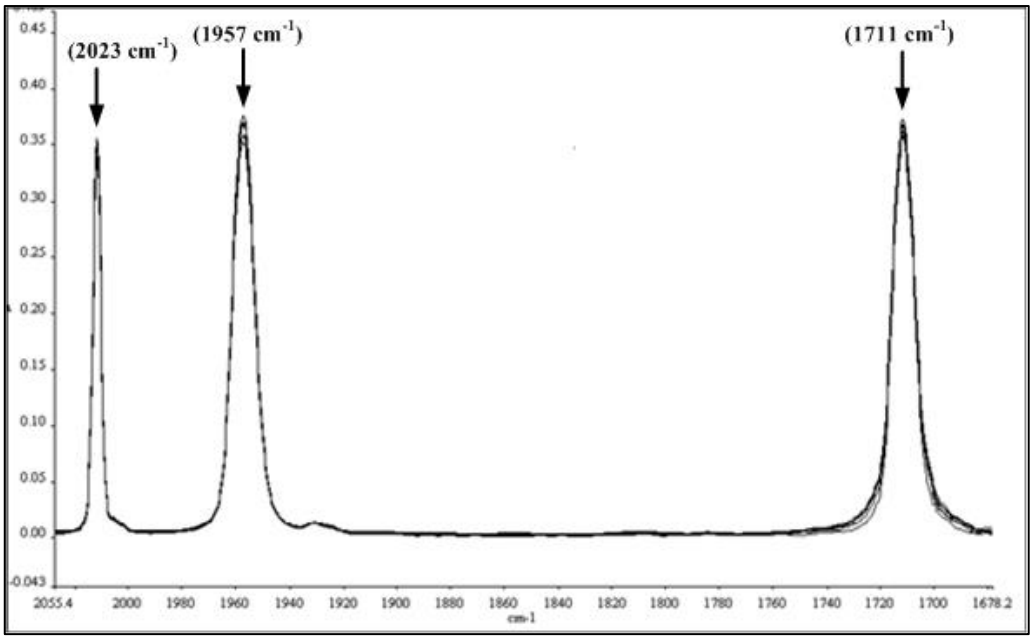

Figure 3-2. Infrared spectral changes for thermal decomposition of $(\eta^5\text{-}C_9H_7)Cr(CO)_2(NO)$ complex in dodecane at 140 ^oC.

The activation energy for the decomposition of the complex was obtained by plotting the natural logarithm of the decomposition (k_{obs}) rate constant versus the reciprocal of the absolute temperature (1/T) and it is shown in Figure 3-4.

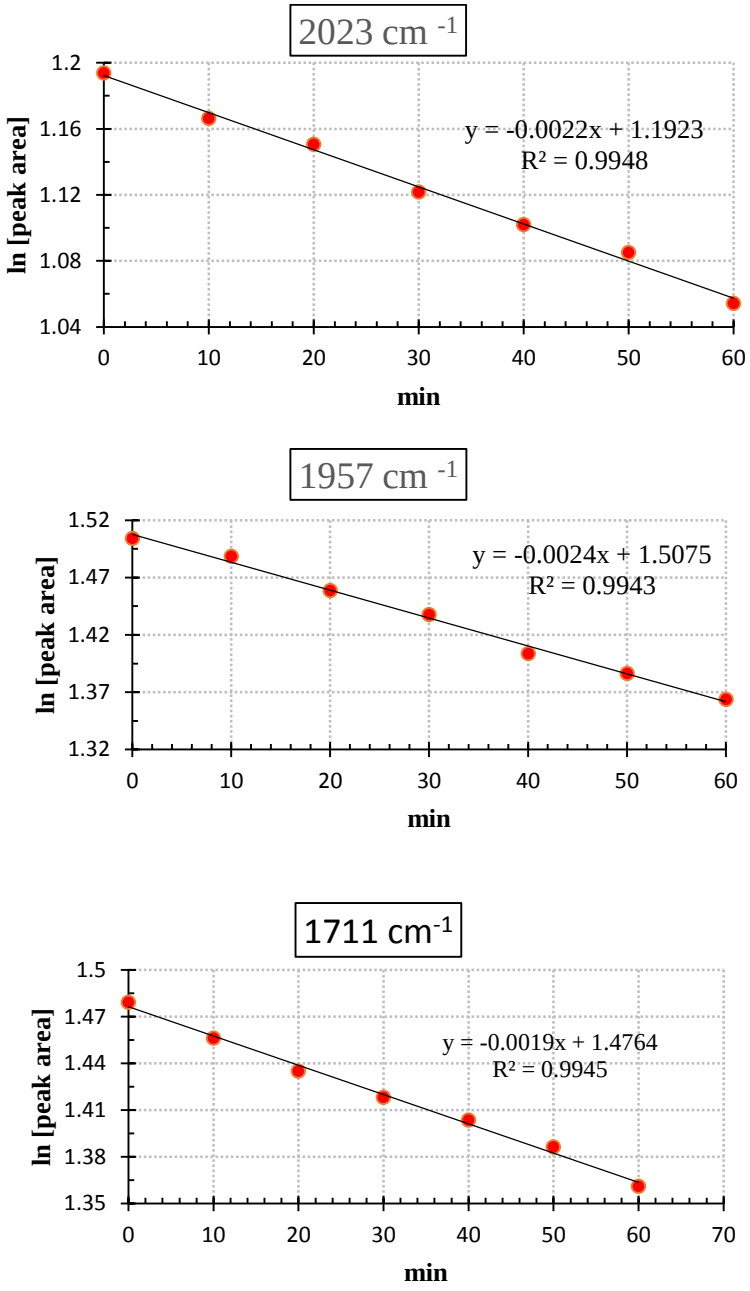

Figure 3-3. Plot of natural logarithm of the peak area of the 2023, 1957, and 1711 cm^{-1} bands of the $(\eta^5\text{-}C_9H_7)Cr(CO)_2(NO)$ versus time. Thermal decomposition of $(\eta^5\text{-}C_9H_7)Cr(CO)_2(NO)$ at 150 °C in dodecane.

Table 3-1.

Data for the $k_{(av)}$ for the thermal decomposition of $(\eta^5\text{-}C_9H_7)Cr(CO)_2(NO)$complex versus temperatures.

Complex	**T(ºC)**	**$k_{(av)}$ Min^{-1}**	**E_a(kJ/mol)**
$(\eta^5\text{-}C_9H_7)Cr(CO)_2(NO)$	180	3.1×10^{-2}	104.9 ±3.81
	150	2.1×10^{-3}	
	140	1.9×10^{-3}	

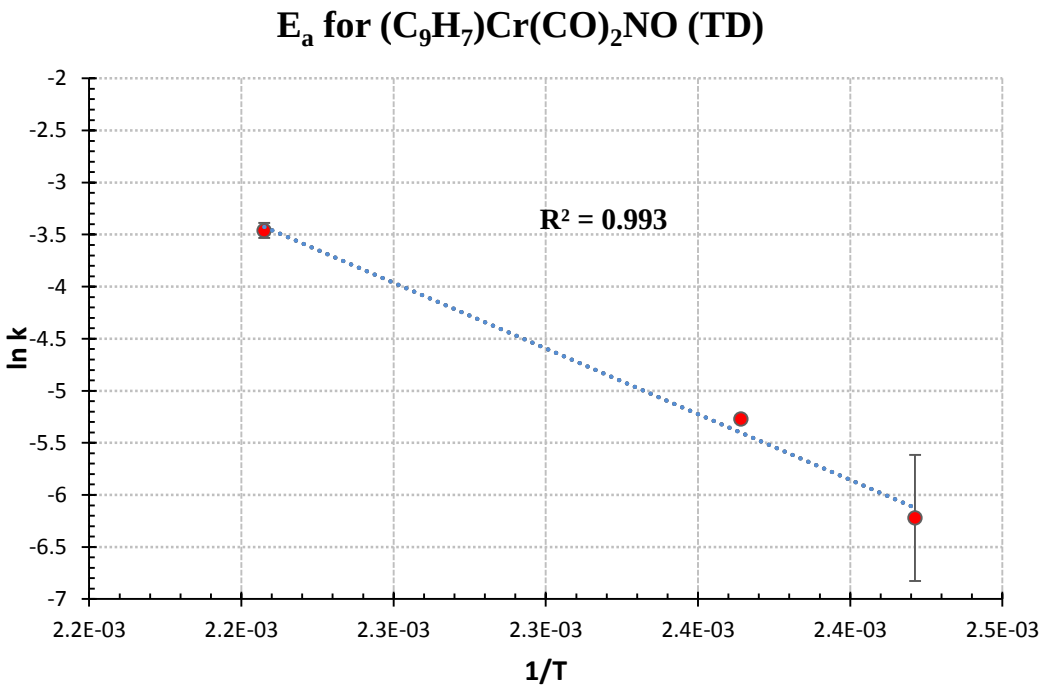

Figure 3-4. Plot of natural logarithm of k_{obs} versus (1/T) (activation energy) of thermal decomposition of $(\eta^5\text{-}C_9H_7)Cr(CO)_2(NO)$complex at 140 to 180 ºC..

3.3.2 Kinetics of ligand substitution in reaction between (η^5-C_9H_7)$Cr(CO)_2(NO)$ and trimethyphosphine, PMe_3, ligand at 85 to 105 °C

The reactions of (η^5-C_9H_7)$Cr(CO)_2(NO)$ with trimethy phosphine PMe_3 in dodecane proceeded according to Equation 3.1 to give the monosubstituted products (η^5-C_9H_7)$Cr(CO)(PMe_3)(NO)$. The product was characterized by IR.

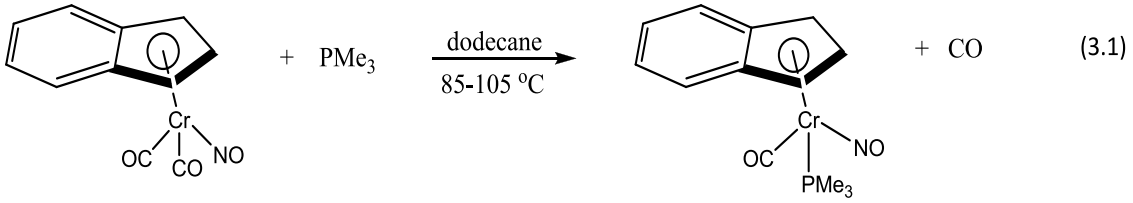

(3.1)

The change of the concentration of the starting material with time has been monitored by IR spectroscopy. Figure 3-5 shows the spectrum over time of disappearance of

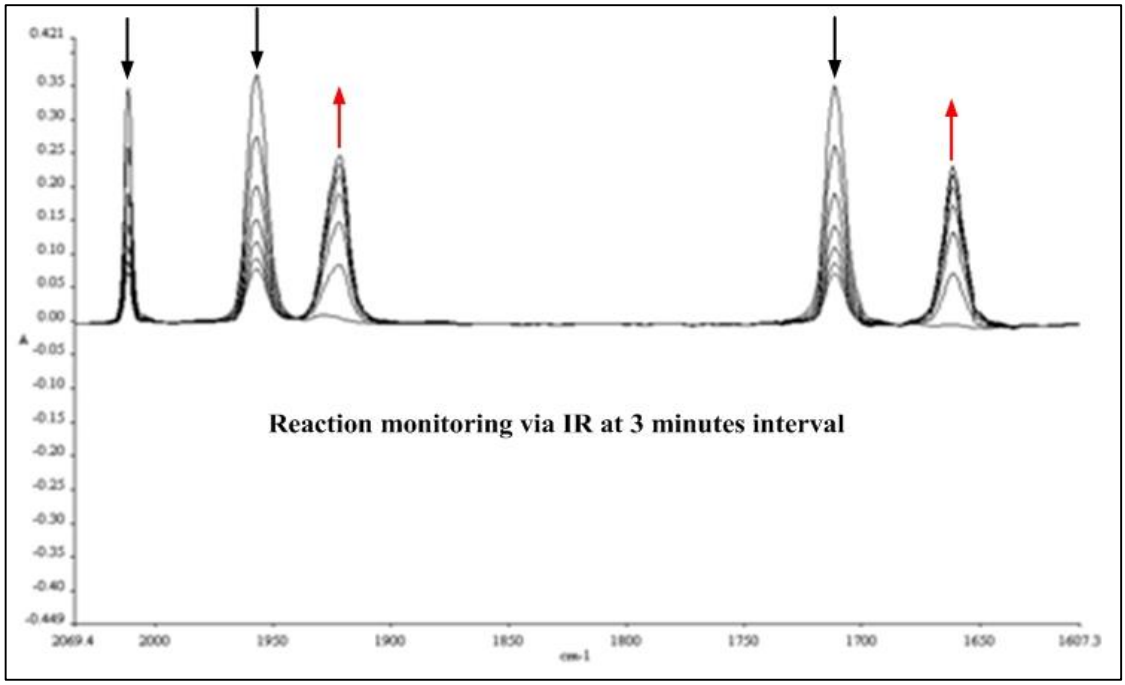

Figure 3-5. Infrared spectral changes for the reaction between (η^5-C_9H_7)$Cr(CO)_2(NO)$ (7.1×10^{-5} M) and PMe_3 (5.4×10^{-3} M) In dodecane at 100 °C..

starting material bands 2023, 1957 and 1711 cm^{-1} of $(\eta^5\text{-}C_9H_7)Cr(CO)_2(NO)$, and appearance of the two bands of monosubstituted product 1914, 1650, cm^{-1} at 100 ^oC. Values of the rate constant k for each run were obtained from slopes of a plot of the natural logarithm of the peak area, ln[A], of the two carbonyl and nitrosyl vibrational bands versus time Figure 3-6. For each temperature at least three kinetic runs were recorded. The rate constants presented in Table 3-2 , Table 3-3 , Table 3-4, Table 3-5 are the arithmetic average of three values of k. The activation energy for the reaction, E_a was obtained by plot of the natural logarithm of the rate constants k_{obs} versus the reciprocal of the absolute temperature (1/T) shown in Figure 3-7. Figure 3-8 shows the value of the two activation parameters the entropy of activation ($\Delta S^{\ddagger}$) and the enthalpy of activation ($\Delta H^{\ddagger}$) and the two parameters were obtained according to the following:

The rate constant is related to the free energy of activation, $\Delta G^{\ddagger}$, by equation (3.2).

$$k = \frac{k'T}{h} e_{RT}^{-\Delta G\ddagger} \qquad (3.2)$$

Where k' is Boltzmann's constant and *h* is Planck's constant. Substituting

$\Delta G^{\ddagger} = \Delta H^{\ddagger} - T\,\Delta S^{\ddagger}$ Gives

$$k = \frac{k'T}{h} e_{RT}^{-\Delta H\ddagger} e_{R}^{\Delta S\ddagger} \qquad (3.3)$$

Rearranging and taking the logarithm gives:

$$ln_T^k = \frac{-\Delta H\ddagger}{RT} + ln_h^{k'} + \frac{\Delta S\ddagger}{R} \qquad (3.4)$$

Plot of ln(k/T) versus (1/T) gives $\Delta H^{\ddagger}$ from the slope and $\Delta S^{\ddagger}$ from the intercept. This type of plot is called an Eyring plot.[3] Table 3-6 shows the average value of both activation parameters for the reaction of $(\eta^5\text{-}C_9H_7)Cr(CO)_2(NO)$ with PMe_3, $PPhMe_2$, PBu_3 and $P(OMe)_3$.

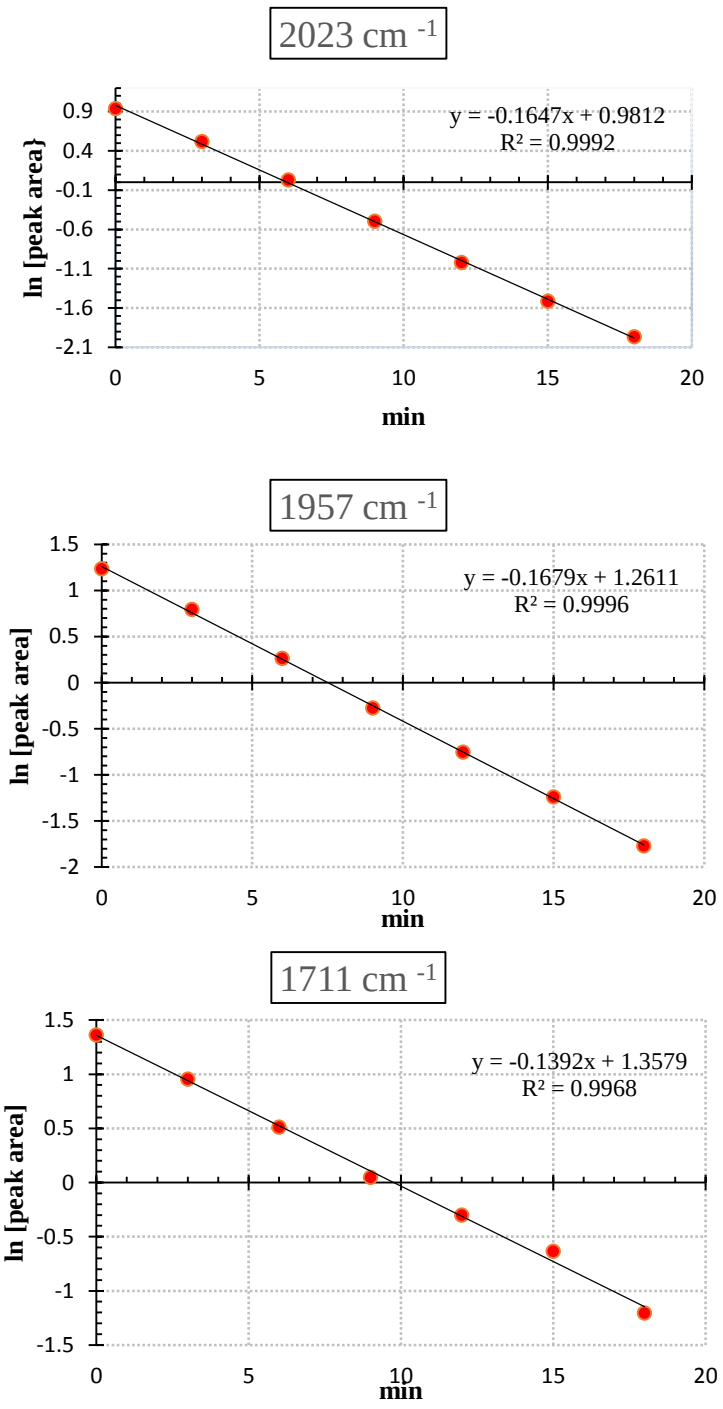

Figure 3-6. Plot of natural logarithm of peak area of 2023, 1957 and 1711 cm^{-1} bands of $(\eta^5\text{-}C_9H_7)Cr(CO)_2(NO)$ versus time. Reaction takes place between $(\eta^5\text{-}C_9H_7)Cr(CO)_2(NO)$ and PMe_3 in dodcane at 100 °C.

Table 3-2.

Data for the $k_{(av)}$ for the reactions of $(\eta^5\text{-}C_9H_7)Cr(CO)_2(NO)$ with PMe_3 ligand at different temperatures in dodecane. Temperature changed from 85 to 105 °C.

Complex	**Ligand**	**T(°C)**	**$k_{(av)}$ min^{-1}**
$(\eta^5\text{-}C_9H_7)Cr(CO)_2(NO)$	PMe_3	105	17.1×10^{-2}
		100	15.5×10^{-2}
		95	11×10^{-2}
		90	9×10^{-2}
		85	8×10^{-2}

Table 3-3.

Data for the $k_{(av)}$ for the reactions of $(\eta^5\text{-}C_9H_7)Cr(CO)_2(NO)$ with $PPhMe_2$ ligand at different temperatures in dodecane. Temperature changed from 95 to 115 °C.

Complex	**Ligand**	**T(°C)**	**$k_{(av)}$ min^{-1}**
$(\eta^5\text{-}C_9H_7)Cr(CO)_2(NO)$	$PPhMe_2$	115	28×10^{-2}
		110	20×10^{-2}
		105	14×10^{-2}
		100	10×10^{-2}
		95	8.3×10^{-2}

Table 3-4.

Data for the $k_{(av)}$ for the reactions of $(\eta^5\text{-}C_9H_7)Cr(CO)_2(NO)$ with PBu_3 ligand at different temperatures in dodecane. Temperature changed from 125 to 145 °C

Complex	**Ligand**	**T(°C)**	**$k_{(av)}$ min^{-1}**
$(\eta^5\text{-}C_9H_7)Cr(CO)_2(NO)$	PBu_3	145	17.1×10^{-2}
		140	14.8×10^{-2}
		135	11×10^{-2}
		130	7.4×10^{-2}
		125	6.3×10^{-2}

Table 3-5.

Data for the $k_{(av)}$ for the reactions of $(\eta^5\text{-}C_9H_7)Cr(CO)_2(NO)$ with $P(OMe)_3$ ligand at different temperatures in dodecane. Temperature changed from 135 to 150 °C

Complex	**Ligand**	**T(°C)**	**$k_{(av)}$ min^{-1}**
$(\eta^5\text{-}C_9H_7)Cr(CO)_2(NO)$	$P(OMe)_3$	150	5.9×10^{-2}
		145	4×10^{-2}
		140	3.7×10^{-2}
		135	3.3×10^{-2}
		130	1.8×10^{-2}

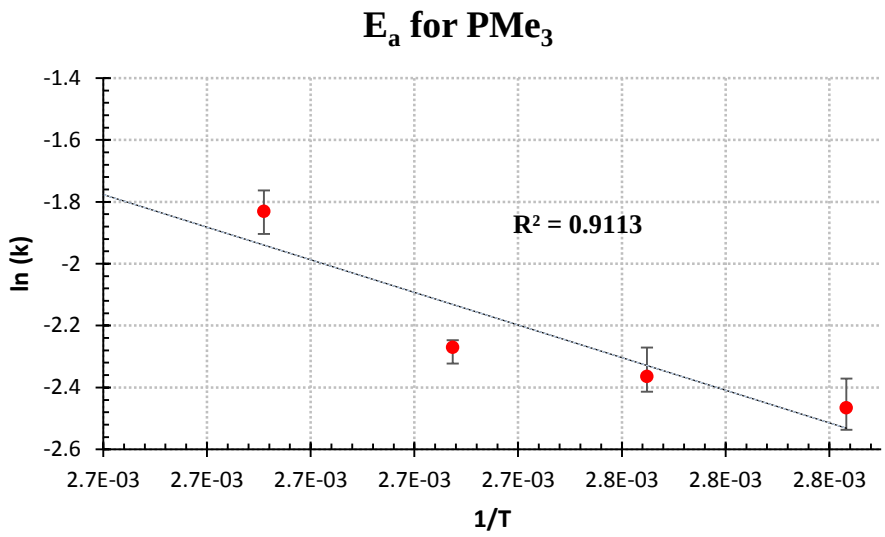

Figure 3-7. Plot of natural logarithm of (k_{obs}) versus (1/T) (activation energy) of the reaction between (η^5-C_9H_7)$Cr(CO)_2(NO)$ and PMe_3 at 85 to 105 °C.

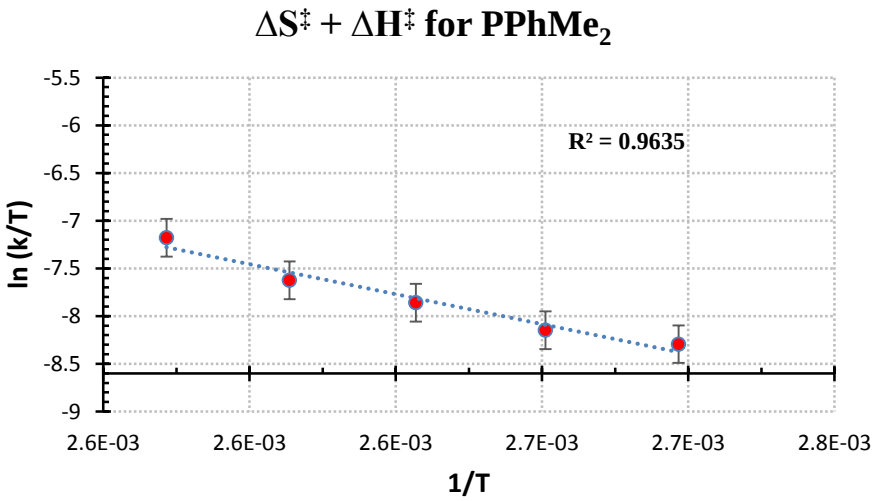

Figure 3-8. Plot of natural logarithm of (k/T) versus (1/T) (activation entropy and activation enthalpy) of the reaction between (η^5-C_9H_7)$Cr(CO)_2(NO)$ and $PPhMe_2$ at 95 to 115 °C

Table 3-6.

Values of enthalpy ($\Delta H^{\ddagger}$) and entropy ($\Delta S^{\ddagger}$) and energy of activation (E_a) for the reaction of $(\eta^5\text{-}C_9H_7)Cr(CO)_2(NO)$ with PMe_3, $PPhMe_2$, PBu_3 and $P(OMe3)_3$ in dodecane

Complex	**Ligand**	**E_a KJ/Mol**	**$\Delta S^{\ddagger}$ eu**	**$\Delta H^{\ddagger}$ (Kcal/mol)**
$(\eta^5\text{-}C_9H_7)Cr(CO)_2(NO)$	PMe_3	42±0.99	-42.3±2.6	39.8±1.0
	$PPhMe_2$	67.15±1.2	-44.1±3.1	49±1.8
	PBu_3	74.6±1.7	-48.4±1.4	54.1±2.5
	$P(OMe)_3$	84.65±2.4	-49.3±2.2	59.1±3.4

3.3.3 Study of concentration effects of $P(OMe)_3$ ligand on the reaction rate between the ligand and $(\eta^5\text{-}C_9H_7)Cr(CO)_2(NO)$ complex

The reaction of $(\eta^5\text{-}C_9H_7)Cr(CO)_2(NO)$ complex with different concentration of the four phosphorus ligands PMe_3, $PPhMe_2$, PBu_3 and $P(OMe)_3$ were done in dodecane at constant temperatures. The results of the rate constant k_{obs} versus concentration were shown in Table 3-7, Table 3-8, Table 3-9, Table 3-10. Figure 3-9 shows the disappearance of the starting material bands and appearance of the monosubstituted products bands. The relation between the rate constant k_{obs} values and the different concentration ligand was shown in Figure 3-10. The value of rate constant was represented in Figure 3-11.

Table 3-7.

Data for the k_{obs} (average) for the reactions of $(\eta^5\text{-}C_9H_7)Cr(CO)_2(NO)$ (7.1×10^{-5} M) with PMe_3 ligand at different PMe_3 concentration at 100 °C temperatures

Complex	**Ligand**	**PMe_3 [M]**	**$k_{(obs)}$ min^{-1}**
$(\eta^5\text{-}C_9H_7)Cr(CO)_2(NO)$	PMe_3	3.9×10^{-4}	4.48×10^{-2}
		6.5×10^{-4}	8.86×10^{-2}
		7.8×10^{-4}	9.13×10^{-2}
		13.1×10^{-4}	15.1×10^{-2}

Table 3-8.

Data for the k_{obs} (average) for the reactions of $(\eta^5\text{-}C_9H_7)Cr(CO)_2(NO)$ (7.1×10^{-5} M) with $PPhMe_2$ ligand at different $PPhMe_2$ concentration at 100 °C temperatures

Complex	**Ligand**	**$PPhMe_2$ [M]**	**$k_{(obs)}$ min^{-1}**
$(\eta^5\text{-}C_9H_7)Cr(CO)_2(NO)$	$PPhMe_2$	2.2×10^{-4}	8.5×10^{-2}
		3.6×10^{-4}	10.1×10^{-2}
		5.0×10^{-4}	17.2×10^{-2}
		7.2×10^{-4}	20.21×10^{-2}

Table 3-9.

Data for the k_{obs} (average) for the reactions of $(\eta^5\text{-}C_9H_7)Cr(CO)_2(NO)$ (7.1×10^{-5} M) with PBu_3 ligand at different PBu_3 concentration at 135 °C temperatures

Complex	**Ligand**	**PBu_3 [M]**	**$k_{(obs)}$ min^{-1}**
$(\eta^5\text{-}C_9H_7)Cr(CO)_2(NO)$	PBu_3	5.8×10^{-4}	10.4×10^{-2}
		6.9×10^{-4}	16.7×10^{-2}
		7.4×10^{-4}	17.4×10^{-2}
		11.6×10^{-4}	20.8×10^{-2}

Table 3-10.

Data for the k_{obs} for the reactions of $(\eta^5\text{-}C_9H_7)Cr(CO)_2(NO)$ (7.1×10^{-5} M) with $P(OMe)_3$ ligand at different $P(OMe)_3$ concentration at 135 °C temperatures

Complex	**Ligand**	**$P(OMe)_3$ [M]**	**$k_{(obs)}$ min^{-1}**
$(\eta^5\text{-}C_9H_7)Cr(CO)_2(NO)$	$P(OMe)_3$	4.0×10^{-4}	3.3×10^{-2}
		4.8×10^{-4}	4.4×10^{-2}
		6.4×10^{-4}	4.6×10^{-2}
		8.0×10^{-4}	6.9×10^{-2}

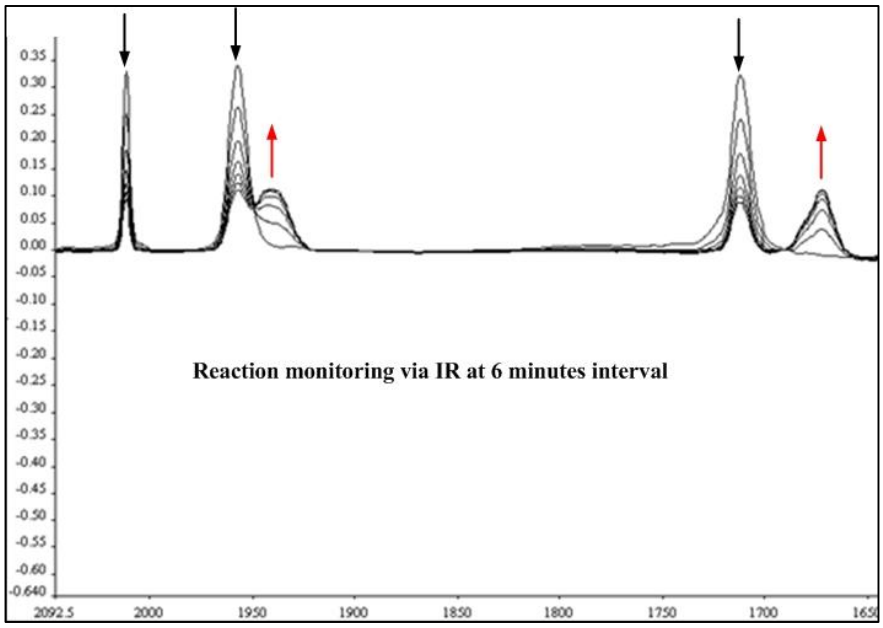

Figure 3-9. Infrared spectral changes for the reaction between $(\eta^5\text{-}C_9H_7)Cr(CO)_2(NO)$ and $P(OMe)_3$ in dodecane at 135 °C when the concentration of $P(OMe)_3$ equal 6.4 x 10^{-4} M.

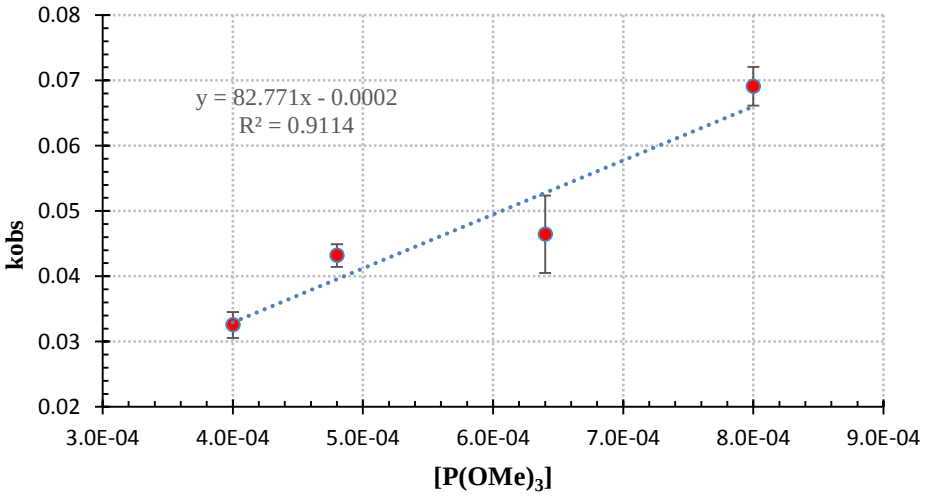

Figure 3-10. Plot of k_{obs} versus $P(OMe)_3$ concentration for the reaction of $(\eta^5\text{-}C_9H_7)Cr(CO)_2(NO)$ with $P(OMe)_3$ in dodecane at 135 °C. Concentration of $P(OMe)_3$ changed from (4.0 x 10^{-4}, 4.8 x 10^{-4}, 6.4 x 10^{-4} and 8.0 x 10^{-4} M)

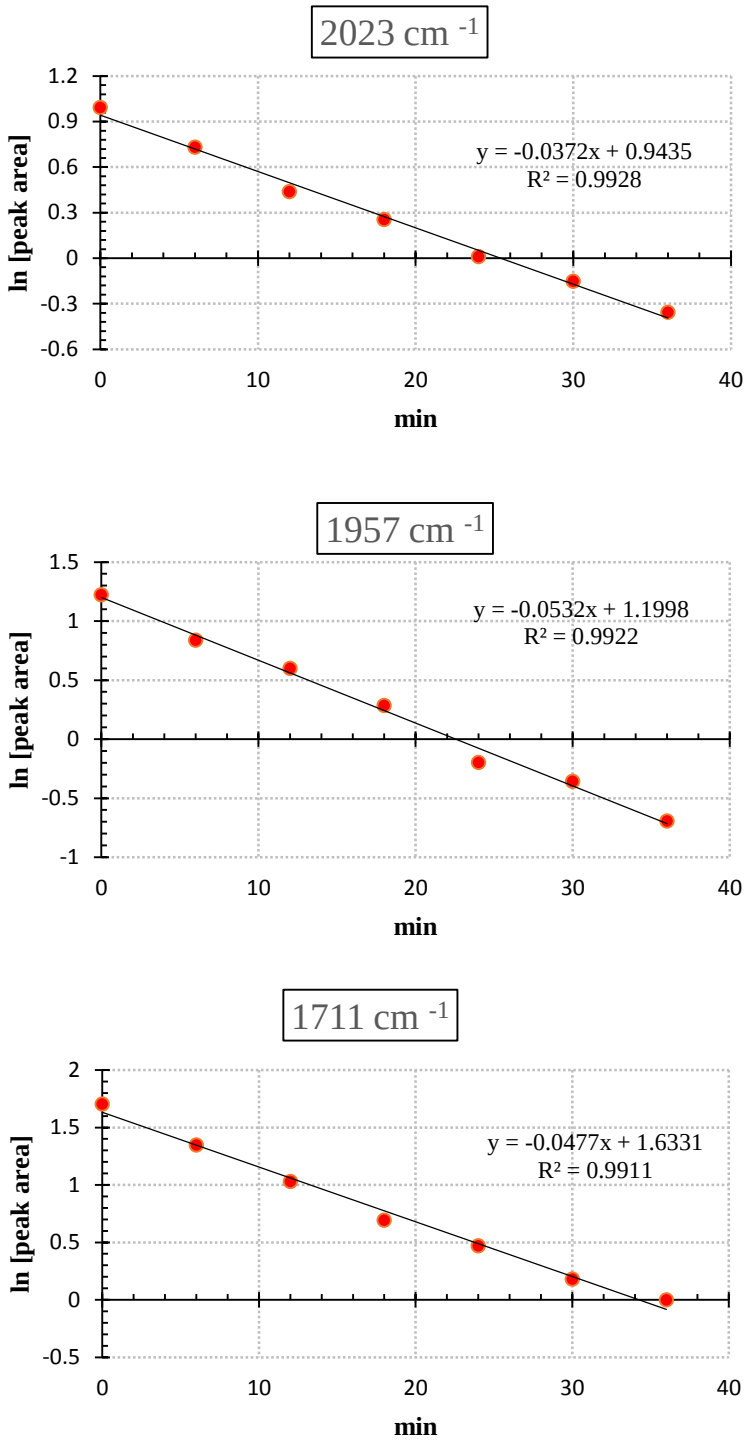

Figure 3-11. Plot of natural logarithm of peak area of 2023, 1957 and 1711 cm^{-1} bands of $(\eta^5\text{-}C_9H_7)Cr(CO)_2(NO)$ versus time. Reaction takes place between $(\eta^5\text{-}C_9H_7)Cr(CO)_2(NO)$ and $P(OMe)_3$ (6.4 x 10^{-4} M) in dodcane at 135 ^oC.

3.4 References

1) Henri, B. *J*. Or*ganometal*. *Chem*. **1968**, 16,119-124.

2) Charles, P. C.; William, D. J.; Stephan, H. *J*. Or*ganometal*. *Chem*. **1981**, 206,38-42.

3) Atwood, J. A. (**1985**). *Inorganic and Organometallic Reaction Mechanisms*. Belmont, CA: Wadsworth.

CHAPTER 4 Results and Discussion of the Kinetic Study for the Reaction of (η^5-C_9H_7)$Cr(CO)_2(NO)$ with Phosphorus ligands

4.1 Introduction

In the previous Chapter we presented the kinetics results of the reaction between (η^5-C_9H_7)$Cr(CO)_2(NO)$ with four phosphorus ligands PMe_3, $PPhMe_2$, PBu_3 and $P(OMe)_3$.The reactions were run at different temperatures and different concentrations of the ligands in order to find the effects of these two factors on the rate. Additionally, the rate of thermal decomposition of.(η^5-C_9H_7)$Cr(CO)_2(NO)$ was determined at three different temperatures in the dodecane solvents. In this chapter we will explore the results of the study to find out if the indenyl ligand or nitrosyl ligands have any effects on the reaction rate of the above reactions.

4.2 Results

Carbon monoxide substitution in (η^5-C_9H_7)$Cr(CO)_2(NO)$ by phosphines and phosphites proceeds readily at different temperatures ranging from 125 to 145 ^oC for PBu_3 , 130 to 150 ^oC for $P(OMe_3)_3$, 95 to 115 ^oC for $PPhMe_2$ and 85 to 105 ^oC for the PMe_3 ligands in dodecane solutions. These reactions can be monitored conveniently by observing changes in the infrared spectra of the carbonyl and nitrosyl bands of the complex as a function of time. All reactions obey the second-order rate law given in Equation 4.1.

$$-d[(C_9H_7)Cr(CO)_2(NO)]/dt = k[(C_9H_7)Cr(CO)_2(NO)][L] \quad (4.1)$$

Rate constants and activation parameters for the various reactions are listed in Tables 3.2, 3.3, 3.4, 3.5 and 3.6. Monosubstitution products were identified by their IR spectra as shown in Table 4-1.

Table 4-1.

Infrared carbonyl and nitrosyl absorptions of reaction products in dodecane

Compound	**cm^{-1}**
$(\eta^5\text{-}C_9H_7)Cr(CO)(PMe_3)(NO)$	1914, 1650
$(\eta^5\text{-}C_9H_7)Cr(CO)(PPhMe_2)(NO)$	1915, 1649
$(\eta^5\text{-}C_9H_7)Cr(CO)(PBu_3)(NO)$	1918, 1659
$(\eta^5\text{-}C_9H_7)Cr(CO)[P(OMe)_3](NO)$	1934, 1663

Decomposition of these species under the conditions of the kinetics studies precluded their isolation and more detailed characterization. The rate of CO substitution increases with temperature and followed the general thumb rule of rate doubling with a temperature increase of 10 ^oC. The data in Tables 3.7, 3.8, 3.9 and 3.10 further demonstrate a doubling of rate with a doubling of ligand concentration consistent with the reaction being first-order in ligand. Thermal decomposition of $(\eta^5\text{-}C_9H_7)Cr(CO)_2(NO)$ was also examined at three different temperatures by following the carbonyl and nitrosyl band integrations. No identifiable product could be observed in these decomposition studies. The rate of thermal decomposition was found to be less than 10% of the ligand exchange rates so no corrections have been made to compensate for this side reaction.

4.3 Discussions

Thermal carbon monoxide substitutions in $(\eta^5\text{-}C_9H_7)Cr(CO)_2(NO)$ by the phosphorus ligands, PMe_3, $PPhMe_2$, PBu_3 and $P(OMe)_3$, depend directly on the concentration of the incoming ligands as shown in Tables 3.7, 3.8, 3.9, and 3.10. The second order character of the reactions and strongly negative values for $\Delta S^{\ddagger}$ support an associative mechanism.

The associative nature of the reactions is further corroborated by the variation of the rate with the nature of the nucleophiles. The relative rates of the various ligands from Tables 3.2,3.3,3.4 and 3.5 show the order of reactivity to be $PMe_3 > PPhMe_2 > PBu_3 > P(OMe)_3$

Several authors have developed experimental methods to measure the nucleophilicity of phosphines and phosphites. In a series of papers, workers at the American Cyanamid Co[1] studied the basicity and nucleophilicity of phosphines. Basicity was measured by titration in nonprotic solvents, while the nucleophilicity was determined by reaction of phosphines with various alkyl halide derivatives. Somewhat later, Drago[2-4] and coworkers developed a two parameter equation to evaluate the electrostatic, E_B, and covalent, C_B, contributions of these ligands. Various values are presented in Table 4-2. These measures give an approximate order of: $PMe_3 \approx PBu_3 > PPhMe_2 > P(OMe)_3 > PPh_3$. Basolo et al.[5,6] measured the rates of reactions of phosphines with $(\eta^5\text{-}C_9H_7)Mn(CO)_3$ and $Co(CO)_3NO$ and found the order of reactivity to be $PPhMe_2 > PBu_3 > P(OEt)_3 > PPh_3$ and $PBu_3 > PPh_2Et_2 > P(OME)_3 > PPh_3$, respectively. These reactions provide clear examples of the "indenyl" and "nitrosyl" effects. The reversal of PBu_3 and $PPhMe_2$ (or $PPhEt_2$) may be reflective of steric differences between the indenyl ring on the one hand and the relatively unencumbered, tetrahedral $Co(CO)_3(NO)$ on the other. The order found in the current work $PMe_3 > PPhMe_2 > PBu_3 >$

$P(OMe)_3$, parallels that of $(\eta^5\text{-}C_9H_7)Mn(CO)_3$ suggesting that the smaller cone angle of $PPhMe_2$ (122^o) vs. PBu_3 (132^o), Table 4-3, dominates over the grater nucleophilicity of PBu_3.

Table 4-2.

The E_B and C_B parameters for phosphines [2]

Ligand	E_B	C_B
PBu_3	0.294	5.90
PMe_3	0.247	5.81
$PPhMe_2$	0.273	5.27
$P(OMe)_3$	0.131	4.83
PPh_3	0.301	4.07

Table 4-3.

The cone angle of some phosphines and phosphite ligands

Ligand	Cone angle (deg)
$P(OMe)_3$	107
PMe_3	118
PMe_2Ph	122
PBu_3	132
PPh_3	145

Table 3.6 shows the value of activation energy E_a for each reaction of the metal complex and increasing in the order PMe_3 > $PPhMe_2$ > PBu_3 > $P(OMe)_3$ based on observed relative rates. The rate constants of the reactions of the $(\eta^5\text{-}C_9H_7)Cr(CO)_2(NO)$ complex with the above ligands derived graphically from the plot of natural logarithm of peak area of the metal complex versus time. This rate constant is a measure of the rate of reaction under pseudo first order conditions. The plot of k_{obs} versus ligand concentration gave a straight line with intercept very close to zero for the four ligands as shown in Figure 4-1.

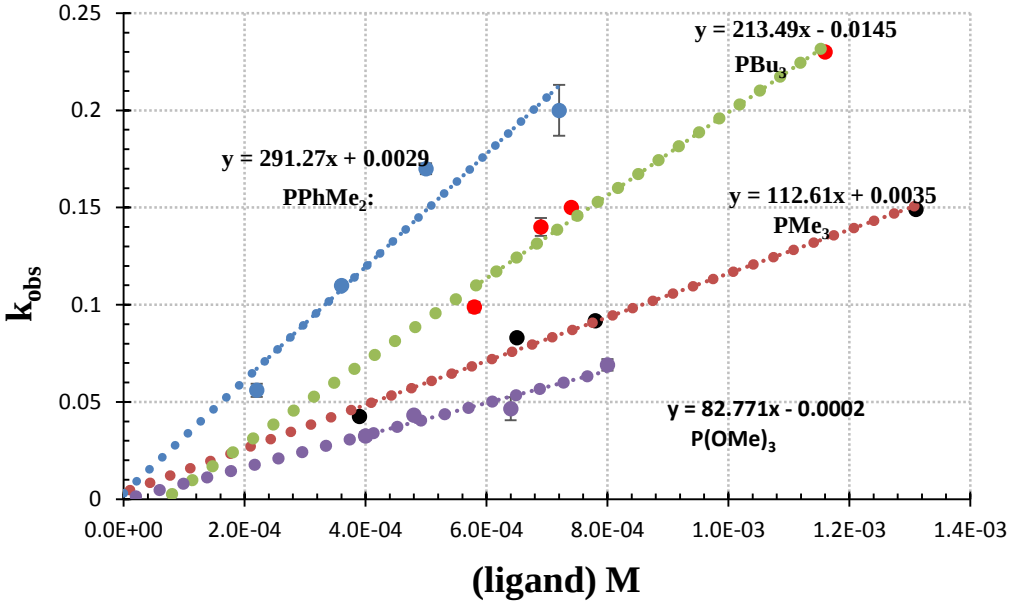

Figure 4-1. Plot of k_{obs} (M^{-1}) versus ligand concentration for the reaction of $(\eta^5\text{-}C_9H_7)Cr(CO)_2(NO)$ with PMe_3, $PPhMe_2$, PBu_3 and $P(OMe)_3$ in dodecane.

The zero intercepts indicate there is no detectable dissociative reaction and the mechanisms of those reactions are mostly associative. A similar observation was made by Basolo[4], et al. in the reaction of $(\eta^5\text{-}C_9H_7)Mn(CO)_3$ as shown in Figure 4-2.

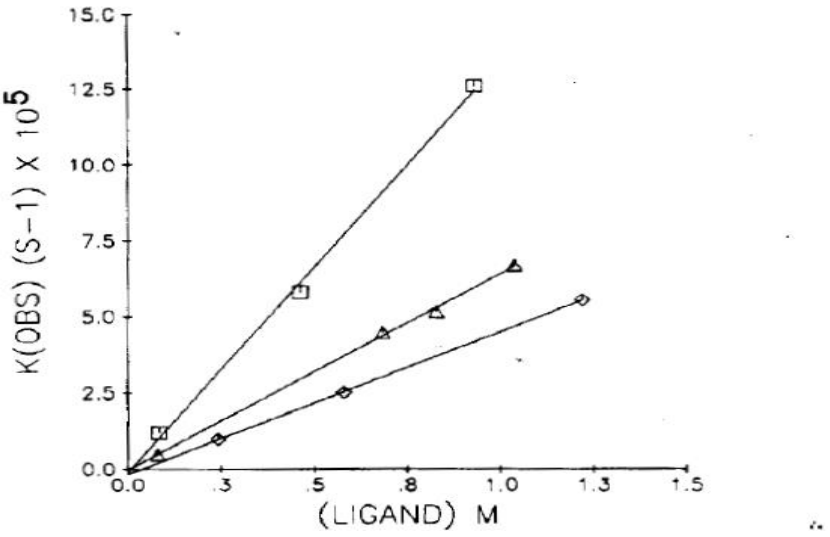

Figure 4-2. Plot of kobs versus PR_3 concentration for the reaction of $Mn(\eta^5\text{-}C_9H_7)(CO)_3$ with different PR_3 [PBu_3 and $P(OEt)_3$] concentration in decaline at different temperatures.[3]

The activation parameters reported by Basolo are presented in table in Table 4-4.

Table 4-4.
Basolo rate constants and activation parameters for the substitution reaction of $Mn(\eta^5\text{-}C_9H_7)(CO)_3$ complex with PBu_3 and $P(OEt)_3$ ligands in decalin.

Complex	**Ligand**	**T °C**	**k s^{-1}**	**$\Delta H^{\ddagger}$ (kcal/mol)**	**$\Delta S^{\ddagger}$ eu**
$Mn(\eta^5\text{-}C_9H_7)(CO)_3$	PBu_3	121	4.04×10^{-5}	17±0.6	-36±1.5
		130	6.46×10^{-5}		
		143	1.34×10^{-5}		
	$P(OEt)_3$	121	2.75×10^{-5}	16±0.7	-37±1.8
		130	4.69×10^{-5}		
		143	7.7×10^{-5}		

While our kinetics results are in Table 4-5

Table 4-5.
Rate constants and activation parameters for the substitution reaction of $(\eta^5\text{-}C_9H_7)Cr(CO)_2(NO)$ complex with PBu_3 and $P(OMe)_3$ ligands in dodecane.

Complex	**Ligand**	**T °C**	**k M^{-1}**	**$\Delta H^{\ddagger}$ (kcal/mol)**	**$\Delta S^{\ddagger}$ eu**
$(\eta^5\text{-}C_9H_7)Cr(CO)_2(NO)$	PBu_3	125	6.3×10^{-2}	54±2.5	-48±1.4
		130	7.4×10^{-2}		
		140	14.8×10^{-2}		
	$P(OMe)_3$	130	1.8×10^{-2}	59±3.4	-49±2.4
		135	3.3×10^{-2}		
		140	3.7×10^{-2}		

4.4 Conclusion

The work presented in this dissertation was initiated with the goal of understanding kinetics of reaction of known chromium indenyl nitrosyl $(\eta^5\text{-}C_9H_7)Cr(CO)_2(NO)$ complex with a set of representative phosphine and phosphite ligands PMe_3. $PPhMe_2$, PBu_3, and $P(OMe)_3$. These results provide unambiguous evidence for rate acceleration in this class of compounds, but distinguishing between the relative contribution of "indenyl" and "nitrosyl" effects is not possible. Future planned studies on $(\eta^5\text{-}C_5H_5)Cr(CO)_2(NO)$ should make it possible to isolate the "nitrosyl" effects.

4.5 References

1) (a) Henderson, W. A.; Streuli. C. A. *J. Am. Chem. Soc*. **1960**, 82, 5791-94. (b) Henderson. W. A.; Buckler. S. A.; *J. Am. Chem. Soc*. **1960**, 82, 5794-5800.
2) Steven, J.; Drago. R. S.; Sales. J. *Organometallics*. **1998**, 17, 589-599.
3) Drago. R. *Organometallics*. **1995**, 14, 3408-17
4) Drago, R.; Joerg. S. *J. Am. Chem. Soc*. **1996**, 118, 2654-63
5) Thorsteinson, E. M.; Basolo, F. *J. Am. Chem. Soc*. **1966**, 88, 3929-36.
6) Ji, L. N.; Rerek, M. E.; Basolo, F. *Organometallic*. **1984**, 3, 740-745.